

A multi-proxy approach to reconstruct hydrological changes and Holocene climate development of Nam Co, Central Tibet

I. Mügler · G. Gleixner · F. Günther · R. Mäusbacher ·
G. Daut · B. Schütt · J. Berking · A. Schwalb ·
L. Schwark · B. Xu · T. Yao · L. Zhu · C. Yi

Received: 28 January 2008 / Accepted: 8 July 2009 / Published online: 13 August 2009
© The Author(s) 2009. This article is published with open access at Springerlink.com

Abstract Holocene lake level fluctuations were reconstructed from a 2.7-m sediment core from Nam Co, Central Tibet, China dating to >7.2 cal ka BP. Results were compared to existing lake records from the Tibetan Plateau to infer variations in the strength of the Asian Monsoon. Geomorphological features in the Nam Co catchment, such as beach ridges and lake terraces, indicate high lake stands during the late Glacial. A major low stand is suggested for the Last Glacial Maximum (LGM). Sands and sandy silts at the base of the core are transgressive facies, with material transported by

melt water and deposited under rising lake level conditions that followed the LGM low stand. Variations in grain size, major elements, biomarker stable isotopes and minerals in the core suggest a climate evolution reflected in at least five depositional units and subunits. Sediments in *Unit I* (~7.2 to ~5.4 cal ka BP) were deposited at highest lake levels. Large amounts of allogenic minerals and allochthonous organic matter suggest high precipitation and melt water input, implying positive water balance. Increasing aquatic productivity points to favourable environmental conditions. *Unit II* (~5.4 to ~4.0 cal ka BP) marks a transition between favourable, stable hydrological conditions and lake level decrease. Lower lake levels were a consequence of drier climate with less monsoonal precipitation, higher evaporation rates, and increased moisture recycling in the catchment. *Unit III* (~4.0 to ~1.4 cal ka BP) reflects the driest periods recorded, at ~3.7 cal ka BP and 1.6 cal ka BP. Lake shrinkage and salinization was interrupted as suggested by the deposition of *Unit IV* (~1.4 to ~0.8 cal ka BP), when increased precipitation and runoff that might be related to the Medieval Warm Period, led to a stable, but still low lake level. *Unit V* (800 cal years BP—present) is characterized by progressive lake shrinkage due to intense evaporation. Large fluctuations in geochemical variables indicate humid and arid periods, respectively, at Nam Co between ~450 and ~200 cal years BP, with the latter assumed to correspond to the Little Ice Age. Modern hydrological

I. Mügler · G. Gleixner (✉) · F. Günther
Max-Planck-Institut für Biogeochemie, Jena, Germany
e-mail: gerd.gleixner@bgc-jena.mpg.de; gglex@bgc-jena.mpg.de

F. Günther · R. Mäusbacher · G. Daut
Friedrich Schiller Universität Jena, Jena, Germany

B. Schütt · J. Berking
Freie Universität Berlin, Berlin, Germany

A. Schwalb
Technische Universität Braunschweig, Braunschweig,
Germany

L. Schwark
Universität Köln, Cologne, Germany

B. Xu · T. Yao · L. Zhu · C. Yi
Institute for Tibetan Plateau Research (ITPR-CAS),
Beijing, China

data indicate the lake level is rising. Comparison of the Nam Co record with other lake records from the Tibetan Plateau suggests general agreement with the broader picture of Holocene environmental evolution. The timing of dry and wet climate conditions at lake sites across Tibet indicates a gradually decreasing influence of the southern monsoon during the Holocene, from NW to SE. Nevertheless, further research is needed to improve our understanding of Holocene spatio-temporal hydrological variations across the Asian continent.

Keywords Paleolimnology · Paleoclimatology · Sedimentology · Biomarker · Deuterium · Stable isotopes · *n*-Alkane · Monsoon · Carbon · Calcite

Introduction

Numerous studies on lake sediment cores from the Tibetan Plateau aimed to reconstruct spatial and temporal changes of monsoonal variations, which are characterized by fluctuations in precipitation and expansion of monsoonal air masses across the Plateau. Investigations focused mainly on sedimentary facies (Morrill et al. 2006; Wünnemann et al. 2003; Zhai et al. 2006), biological proxies (Herzschuh et al. 2006; Wu et al. 2007), pollen (Chen et al. 2006; Miehe et al. 2006), geochemistry (Wu et al. 2006b), stable isotopes (Fan et al. 2007; Johnson and Ingram 2004; Tian et al. 2007) and paleoshoreline features (Lehmkuhl et al. 2000). The broad picture of Holocene climate evolution is consistent and demonstrates that several warm and dry or wet and cold oscillations occurred, but that their timing, duration, and amplitudes differed across the Tibetan Plateau. In general, during the late Glacial, dry and cold conditions dominated, with weak monsoonal circulation. With the onset of the Holocene, warmer and wetter climate prevailed. The monsoonal circulation strengthened in association with increasing precipitation, relative humidity and temperature. The early Holocene was a period with lake-level high stands and is often referred to as the Holocene Climate Optimum (An et al. 2000). Thereafter, climate became drier and lake levels declined. This is assumed to have been a result of decreasing intensity of monsoonal circulation, implying reduced precipitation, relative humidity, and temperature. The establishment

of modern climate conditions is controversial. Although the general trend to aridity after 4.5 cal ka BP (Gasse et al. 1991) can be deduced from several records (Morrill et al. 2006; Wu et al. 2006b; Wünnemann et al. 2003; Yancheva et al. 2007), other lakes such as Boston Lake in the NW (Herzschuh 2006; Wünnemann et al. 2006), do not display clear aridity trends. Also, stable isotope records from the Dundee and Guliya ice cores indicate gradual warming, but suggest wet conditions for the late Holocene (Thompson et al. 2006; Yao et al. 1997).

A complete picture of Holocene environmental and climate evolution on the Tibetan Plateau is still lacking. Previous paleoclimate studies were done at various locations, but used different climate proxies and were of variable temporal resolution (An et al. 2000; Morrill et al. 2003).

Lake sediments contain geochemical signatures from various sources in the catchment and thus record environmental and hydrological changes controlled by climate variations (Leng and Marshall 2004; Meyers and Lallier-Verges 1999; Morrill et al. 2006). Autochthonous organic matter and authigenic carbonates reflect in situ lake conditions. Allochthonous organic materials originate from terrestrial plants and authigenic minerals, which are transported into the lake, and indicate environmental conditions in the catchment.

In this study, lacustrine sediments were analysed to assess lake level changes in Nam Co, Central Tibetan Plateau. Lake level changes are attributed to alternating hydro-climatic conditions and therefore indicate fluctuations in monsoon strength (Lehmkuhl and Haselein 2000; Morrill 2004). We present results inferred from grain size distribution, major elements, stable isotopes and minerals. Furthermore, compound-specific hydrogen isotope ratios (δD values) in lacustrine *n*-alkanes were measured. These biomarkers of known origin provide information on climate and vegetation change. Long-chain *n*-alkanes with a predominant odd carbon number (nC_{25} – nC_{33}) are abundant components of vascular plant epicuticular waxes (Eglinton and Hamilton 1967). *n*-alkanes with 15–19 carbon atoms are synthesized by aquatic bacteria and algae (Cranwell et al. 1987), whereas submerged or floating plants mainly produce *n*-C₂₁ to *n*-C₂₅ compounds (Baas et al. 2000; Ficken et al. 2000). The δD of leaf wax *n*-alkanes tracks δD values of source water, lake water, and precipitation, with an

observed isotopic difference caused by fractionation during *n*-alkane biosynthesis, and additional enrichment in δD of leaf water due to transpiration and evaporation of soil and leaf water in *n*-alkanes of terrestrial plants (Sachse et al. 2006; Smith and Freeman 2006). Drivers of the isotopic composition of precipitation, such as water vapour source, amount of precipitation, air temperature, and relative humidity (Craig 1961; Dansgaard 1964), can be reconstructed from terrestrial biomarker δD values (Sachse et al. 2004; Schefuss et al. 2005; Shuman et al. 2006). Because evapotranspiration enriches δD in the leaf water of terrestrial plants, δD values in *n*-alkanes of terrestrial plants are indicative of the balance between precipitation and evaporation on land (Sachse et al. 2006; Smith and Freeman 2006). Aquatic plants use lake water as a hydrogen source. Nam Co has no outflow, so the δD of lake water is controlled primarily by the balance between precipitation (or melt water) and evaporation. Thus, *n*-alkane δD values from terrestrial vegetation record the hydrogen isotope variations of precipitation. Depleted values reflect high amounts of monsoonal rainfall. Enriched values indicate atmospheric moisture comes from continental sources, such as the Westerlies, or from convective precipitation after evaporation from the lake surface. *n*-Alkane δD values from aquatic organisms record changes in the hydrogen isotope ratios of the lake water, controlled mainly by the balance between evaporation and inputs.

In contrast to many other lake level records from the Tibetan Plateau, the sediment core from Nam Co is continuous and records the drier period of the Late Holocene, which is missing in many other cores (Morrill et al. 2006; Wu et al. 2006a). Thus, even short-term hydrological changes during the last 7 ka are recorded in Nam Co and provide new information on the precipitation/evaporation history of the region, controlled by the strength of the Monsoon system. The Nam Co lake level record is compared to existing lake records across the Tibetan Plateau to reveal the spatio-temporal pattern of monsoonal circulation during the Holocene.

Study site

Nam Co, the second largest, highest saline lake in China, is located in the central part (30°30'–35'N, 90°16'–91°03'E; 4,722 m a.s.l.) of the Tibetan Plateau, about 120 km north of the city of Lhasa (Fig. 1). Climate in this region is semi-arid to semi-humid continental, and modified by altitude. Geographical, climatological and limnological characteristics (Wang and Zhu 2006) are summarized in Table 1. The closed basin is bordered by the Grandise Range in the south, the Nyainqentanglha Range in the southeast, and the Northern Tibetan Plateau hills in the north. Because Nam Co has no outflow, its water balance is controlled by the relation between precipitation and inflow, and evaporation. Several streams, mainly at the SE and SW lake margin, drain into Nam Co and are associated with

Fig. 1 Nam Co and selected lake sites across the Tibetan Plateau discussed in the text, the Nam Co 8 coring site is marked with an *asterisk* (modified, after Jim Knighton, Clear Light Image Products, Copyright 2000)

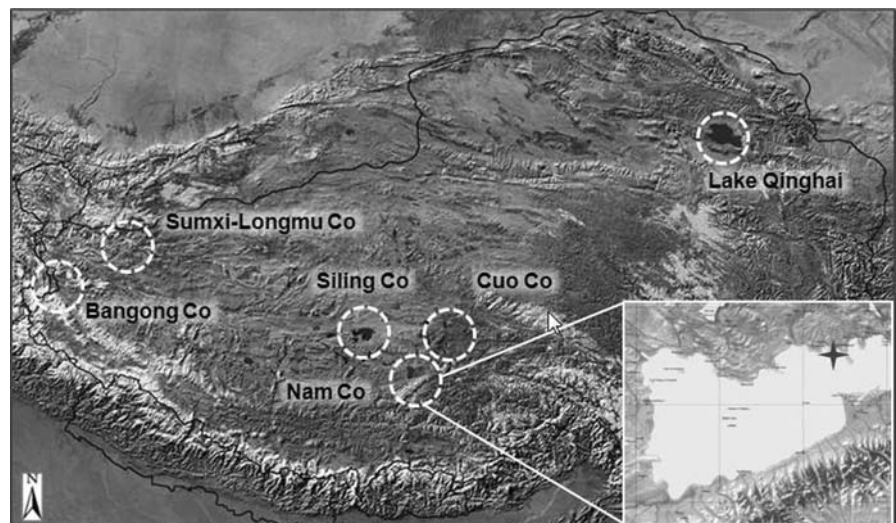


Table 1 General geographical, climatological and limnological data for Nam Co

Altitude	4,722 m a.s.l.
Area	1,920 km ²
N–S	40 km
E–W	75 km
Catchment area	1.06 × 10 ⁴ km ²
Annual precipitation	281 mm (May–October)
Annual evaporation (lake surface)	790 mm
Annual evaporation (terrestrial basin)	320 mm
Annual average temperature	0°C
Annual average relative humidity	52.6%
Maximum water depth	100 m
Ice cover	3–5 months (2 m ice thickness)
pH	9.4
Salinity	2.9–1.3 g/l ⁻¹

wetlands. The Nam Co basin is located in the Lhasa block that was accreted during the Late Jurassic–Early Cretaceous (Kapp et al. 2005). Cretaceous–Tertiary granitoids and orthogneisses are exposed in the southern and southeastern part of the catchment together with Paleozoic to Cretaceous (Dykoski et al. 2005) metasediments of slate, phyllite, limestone and schists, red sandstone, mudstone and conglomerate. Quaternary sediments consist of glacial, fluvial and lacustrine deposits (Zhang et al. 2006). The extent of the glaciers during the Quaternary is still debated.

Alpine steppe and desert soils dominate the northern lake shore. More humid conditions, due to the presence of several rivers, led to the formation of alpine and subalpine meadow soils and marshland soils on the southern bank (Gao 1985).

The vegetation surrounding the lake is typical for an arid, high-altitude climate, and consists primarily of alpine meadows and steppe grasses including species of *Stipa*, *Artemisia*, *Kobresia*, *Oxytropis* and *Morina*. Emergent *Carex* spp., typical in lakes with low salinities, are also found at Nam Co. Bacillariophyta are common in the Nam Co phytoplankton (Williams 1991).

Thirteen lake levels were identified by cliff-lines and beach ridges around Nam Co (Lehmkuhl and Haselein 2000). The highest lake level is marked by a

distinct cliff-line found nearly everywhere around the lake at ~29 m above modern lake level and dated to the late Glacial. The late Glacial and Holocene beach ridges are deposited on top of glacial till or older alluvial fans. Reactivation of channels after lake retreat resulted in dissection of the beach ridges and older fluvial deposits.

Materials and methods

Sampling and lithology

Core Nam Co 8 was collected in the NE basin of Nam Co at 31 m water depth (Fig. 1). The core was retrieved using a piston corer (UWITEC, Mondsee, Austria) and the upper 270 cm were analysed. After splitting lengthwise, the core was photographed and measured for magnetic susceptibility at high-resolution (1 mm steps) using a Bartington MS2E surface-scanning sensor (Bartington, Oxford, England) at the geocological–sedimentological laboratory, University of Jena, Germany. The core has coarse sandy material at the base, followed by a 100-cm-thick, dark-grey layered sequence of silty clay or silt that indicates partial anoxia due to insufficient water column mixing. These layered sediments gradually change in colour from dark grey in the lower part to light grey in the upper part. A dark grey, 20-cm-thick layer with coarse material terminates this sequence at a core depth of ~80 cm. The dark colour is ascribed to a high amount of clastic material. The uppermost part of the core consists again of dark and light grey layered clays or silty clays, indicating reducing conditions during deposition.

Sedimentological and geochemical analyses

The core was sampled at 1-cm intervals. For the following analyses samples were taken at 5- and 2-cm intervals. All samples were freeze-dried and ground for geochemical and biochemical analyses. The samples for grain-size analyses were treated with HCl (15%) and H₂O₂ (15, 30%) to remove carbonates and organic matter, respectively. Grain size was determined with a Beckmann Coulter Laser Diffraction Particle Size Analyser (LS 13320).

Major elements (Na, K, Mg, Fe, Mn, Ca, Sr, Al, P) in bulk sediment and carbonates (Ca, Mg, Sr mainly incorporated in ostracode valves), were analysed after microwave extraction by a modified aqua regia digestion, and by HCl digestion for carbonates. Element concentrations in digestate were measured with an atomic absorption spectrometer (Shimadzu AA 6800). Relative analytical errors ranged from 2 to 10% depending on the element. Total carbon (TC), total organic carbon (TOC), total nitrogen (TN) and total sulphur (TS) were determined with an elemental analyser (Vario EL). The detection limit for CNS analyses was 0.02–0.05% depending on the element. CaCO₃ content was estimated from TC minus TOC, assuming carbonate is calcite.

Mineralogical composition was determined on powder samples by X-Ray Diffraction (PW1710, Philipps,) using a copper $k\alpha$ tube from 2 to 52°2 θ with steps of 0.01° 2 θ , with each step measured for 2 s at the Physical Geography Laboratory, Department of Earth Sciences, FU-Berlin. Contents of mineral components were quantitatively derived from diffraction intensity and peak areas using Philipps X'Pert HighScore software. Accuracy and detection limits were mineral-specific. Compound-specific δ D measurements were performed at 2–3 cm intervals and δ^{13} C analyses at 10 cm intervals. Initially, δ^{13} C was determined on bulk organic matter using an isotope ratio mass spectrometer (IRMS, Delta^{plus}, Finnigan MAT, Bremen, Germany). Sediment was freeze dried and ground. Between 1 and 2 g dry sediment was used for lipid extraction using an accelerated solvent extractor (ASE-200, DIONEX Corp., Sunnydale, USA). The ASE was operated with a dichloromethane: methanol mixture (DCM/MeOH 10:1) at 100°C and 2,000 psi for 15 min in 2 cycles. Activated copper granules were added to the total lipids to remove elemental S. Separation of carboxylic acids and the high polarity fraction was carried out by column chromatography with KOH-silica gel (McCarthy and Duthie 1962). The low polarity fraction was further separated using Medium Pressure Liquid Chromatography (MPLC) with hexane as the only eluent (Radke et al. 1980). A pre-column was filled with deactivated silica gel where the neutral fraction was injected. Aliphatic hydrocarbons were collected after they passed through a main column at a constant flow rate of 8 ml/min. Elution of aromatic

hydrocarbons was carried out by back flushing the main column. The alcohol fraction that remained on the pre-column was eluted with DCM/MeOH (93/7). Volume reduction was performed with a turbo vaporizer (Zymark).

Identification and quantification of *n*-alkanes was accomplished using a GC-FID (TraceGC, Thermo-Electron, Rodano, Italy) by comparison to an external *n*-alkane standard mixture (*n*C₁₀ to *n*C₃₁). The GC was equipped with a DB5 column (30 m, 0.32 mm ID, 0.5 μ m film thickness, Agilent, Palo Alto, USA). The injector (PTV) was operated at 280°C at a constant temperature mode and a split ratio of 1:10. Temperature was held at 80°C for 2 min, and then ramped to 320°C at 8°C min⁻¹. The oven was held at final temperatures for 5 min. The column flow was constant throughout the whole run at 1.8 ml min⁻¹.

Stable isotopes (δ D and δ^{13} C) were determined on *n*-alkanes using a coupled GC-IRMS system (HP5890 GC, Agilent Technologies, Palo Alto USA; IRMS: Delta^{plus} XL, Finnigan MAT, Bremen, Germany). The alkane fraction dissolved in hexane was injected (1 μ l) into a HP5890 GC, equipped with a DB1 ms column (50 m, 0.32 mm ID, 0.52 μ m film thickness, Agilent). The injector was operated at 280°C in the splitless mode. The oven was maintained for 1 min at 50°C, heated at 9°C min⁻¹ to 308°C and held there for 2 min and finally ramped to 320°C at 20° min⁻¹ and held at its final temperature for 3 min. The column flow was constant at 1.7 ml min⁻¹. To monitor possible co-elution of *n*-alkanes with other components, part of the column effluent went to an ion trap mass spectrometer (GCQ ThermoElectron, San Jose, USA). The remainder of the split went to an isotope mass spectrometer, via quantitative conversion to H₂ in a high-temperature oven operated at 1,425°C (Hilkert et al. 1999). Each sample was analysed in triplicate. The isotopic composition of samples is reported in conventional δ -notation, in per mil relative to the VSMOW and VPDB standards for hydrogen and carbon, respectively:

$$\delta^2\text{H}(\delta^{13}\text{C})_{\text{sample}}(\text{‰}) = [(R_{\text{sample}} - R_{\text{standard}})/R_{\text{standard}}] \times 1000$$

where *R* is the ²H/¹H or ¹³C/¹²C ratio of the sample and the standard, respectively. The values in the

standard mixture were calibrated against international reference substances (NBS-22; IAEA-OH22) using offline high-temperature pyrolysis (TC/EA) (Gehre et al. 2004). The average standard deviation (σ) of all $\delta^{13}\text{C}$ measurements was 3.68‰. The accuracy for δD measurements was evaluated using routine measurement of the standard mixture after every six injections (two samples). The average standard deviation (σ) of all measured samples for δD was 8.7‰. If necessary, a drift correction was applied. To ensure stable ion source conditions during measurement, the H^{3+} factor (Hilkert et al. 1999) was determined at least once a day; it was constant over the 10-day measurement period at 5.4 (SD 1.4).

Rock Eval analysis of the powdered sediment (1 mg) was carried out on a VINCI Rock Eval II instrument, applying standard methods at the organic geochemical laboratory in the Institute for Geology and Mineralogy, Cologne University (Espitalie et al. 1985). Results are expressed as the conventional Hydrogen Index (HI—mg hydrocarbons per g TOC) and Oxygen Index (OI—mg Carbon dioxide per g TOC).

Chronology

Core chronology is based on 27 AMS ^{14}C ages determined on bulk sediment sampled at 10-cm intervals and four macroscopic plant remains. Radiocarbon measurement was done at the Max Planck Institute for Biogeochemistry Laboratory, Jena, Germany (Steinhof et al. 2004). Due to the low quantity of plant remains, the radiocarbon ages of three of the plant samples could not be reliably determined. All ^{14}C ages were calibrated with OxCal 4.0 (Bronk Ramsey 2001) and the age-depth relation was established with the mean values of the 2σ error bands (Table 2).

Bulk organic matter from the Nam Co 8 core yielded ^{14}C ages with a nearly linear age-depth relation in the basal 140 cm (120–260 cm) (Fig. 2). Samples in the upper 120 cm all yielded ages of $\sim 2,000$ cal yr BP, with slight increasing ^{14}C ages towards the top of the core. Hard-water effect may account for the anomalous dates. The increase in this effect since $\sim 2,000$ years ago may reflect increased contribution of weathered carbonates or old organic carbon from surrounding wetlands (Smittenberg et al. 2006). The hard-water effect is often assumed to be constant, and for alkaline lakes on the Tibetan

Plateau, reservoir ages between 1,000 and 6,000 ^{14}C years are reported (Fontes et al. 1996; Wu et al. 2006b). Several strategies have been used to correct for the reservoir effect: (1) the ^{14}C age of the surface sample is used to estimate the reservoir effect, (2) a terrestrial plant remain is compared to the bulk ^{14}C age from the same core depth, or (3) the reservoir age is determined from the age/depth linear regression. We used the latter option because a surface sample was not available. This gave a reservoir effect of 949 ^{14}C years (Fig. 2), comparable to the value in other low-salinity lakes on the Plateau (Wu et al. 2006a, b; Xu and Zheng 2003; Zhai et al. 2006). This approach is supported by the AMS- ^{14}C date on aquatic plant remains at 15 cm depth, which lies close to the regression line. We assumed the reservoir effect was constant over time. The Nam Co 8 sequence thus extends back to $\sim 7,300$ cal years BP.

The age-depth relation for Nam Co 8 was established using the regression lines from ^{14}C ages on bulk material from the upper (60–120 cm) and the lower (120–270 cm) core sections. Because ^{14}C ages in the uppermost 60 cm showed age reversals, they were omitted from the age model. Another core from 60 m water also showed reversed ages near the top, supporting our conclusion about changing reservoir effect (Zhu et al. 2007). Mean sedimentation rate for the basal part of the core was 0.26 mm/a, whereas the mean rate for the last 1,000 cal years was 1.19 mm/a. One-cm samples thus integrate 38.4 and 8.4 years, respectively.

Results

Sediment stratigraphy

In general, grain size distribution is fairly uniform in core Nam Co 8, with greyish silt deposits dominating the entire sequence (Fig. 3). However, two major units were distinguished based on grain size. These are the lower core section, where clayey material makes up to 25% of the sediments, and the upper core section, starting from 2.5 cal ka BP, with decreasing clay content and mainly silt. Sand increases occasionally, but never constitutes $> 15\%$ of the grain size. Magnetic susceptibility increases where sand content is higher. Peaks at around 1.5 and 4 cal ka BP are neither reflected in the grain size distribution nor

Table 2 ^{14}C ages from sediment core Nam Co 8

Sample	Pnum	Depth (cm)	Material	^{14}C age (year BP)	Calibrated age (2σ cal year BP)	Mean (cal year BP)	Error (\pm years)
Nam Co 8 C 0-1	2,549	5	OM _{bulk}	2,062 \pm 28	2,117 – 1,949	2,033	119
Nam Co 8 C 10-11	2,550	15	OM _{bulk}	1,902 \pm 26	1,923 – 1,740	1,832	129
Nam Co 8 C 10	1,821	15	Plant r.	905 \pm 25	911 – 743	827	119
Nam Co 8 C 20-21	2,551	25	OM _{bulk}	1,745 \pm 25	1,714 – 1,569	1,642	103
Nam Co 8 C 30-31	2,552	35	OM _{bulk}	1,676 \pm 24	1,690 – 1,527	1,609	115
Nam Co 8 C 40-41	2,553	45	OM _{bulk}	1,844 \pm 37	1,874 – 1,702	1,788	122
Nam Co 8 C 50-51	2,554	55	OM _{bulk}	2,359 \pm 26	2,460 – 2,337	2,399	87
Nam Co 8 C 60-61	2,555	65	OM _{bulk}	1,770 \pm 85	1,896 – 1,447	1,672	317
Nam Co 8 B 70-71	2,556	75	OM _{bulk}	1,541 \pm 59	1,541 – 1,315	1,428	160
Nam Co 8 B 80-81	2,557	85	OM _{bulk}	1,622 \pm 43	1,684 – 1,405	1,545	197
Nam Co 8 B 90-91	2,558	95	OM _{bulk}	1,811 \pm 24	1,821 – 1,637	1,729	130
Nam Co 8 B 100-101	2,559	105	OM _{bulk}	1,992 \pm 24	1,993 – 1,888	1,941	74
Nam Co 8 B 110-111	2,560	115	OM _{bulk}	1,778 \pm 33	1,816 – 1,611	1,714	145
Nam Co 8 B 120-121	2,561	125	OM _{bulk}	3,050 \pm 36	3,364 – 3,162	3,263	143
Nam Co 8 B 130-131	2,562	135	OM _{bulk}	2,756 \pm 32	2,945 – 2,776	2,861	120
Nam Co 8 B 140-141	2,563	145	OM _{bulk}	3,308 \pm 27	3,617 – 3,462	3,540	110
Nam Co 8 B 155-156	2,564	155	OM _{bulk}	3,764 \pm 29	4,236 – 3,997	4,117	169
Nam Co 8 B 160-161	2,565	165	OM _{bulk}	3,717 \pm 33	4,154 – 3,934	4,044	156
Nam Co 8 A 170-171	2,566	175	OM _{bulk}	3,824 \pm 28	4,406 – 4,095	4,251	220
Nam Co 8 A 180-181	2,567	185	OM _{bulk}	4,009 \pm 35	4,570 – 4,415	4,493	110
Nam Co 8 A 190-191	2,568	195	OM _{bulk}	4,253 \pm 32	4,868 – 4,659	4,764	148
Nam Co 8 A 200-201	2,569	205	OM _{bulk}	4,546 \pm 53	5,445 – 4,980	5,213	329
Nam Co 8 A 210-211	2,570	215	OM _{bulk}	5,124 \pm 29	5,932 – 5,753	5,843	127
Nam Co 8 A 220-221	2,571	225	OM _{bulk}	5,563 \pm 41	6,433 – 6,288	6,361	103
Nam Co 8 A 230-231	2,572	235	OM _{bulk}	6,245 \pm 37	7,261 – 7,021	7,141	170
Nam Co 8 A 240-241	2,573	245	OM _{bulk}	6,195 \pm 51	7,248 – 6,968	7,108	198
Nam Co 8 A 250-251	2,574	255	OM _{bulk}	6,847 \pm 37	7,785 – 7,607	7,696	126
Nam Co 8 A 260-261	2,575	265	OM _{bulk}	7,376 \pm 33	8,324 – 8,050	8,187	194

Calibration was performed with OxCal 4.0 using INTCAL 2004 calibration data set. Calibrated ages refer to 2σ results of calibration. Mean ages were used for the age-depth relation of core Nam Co 8

do they appear contemporaneously, because they were determined at lower resolution. Sandy material, interpreted as a melt-water deposit, was found in the basal part of the core. Only the upper, clayey, silt-dominated sequence was considered. However, correlations with other cores and seismic investigations suggest the basal sandy sediment was deposited under very different environmental conditions. Seismic profiles suggest that the coarse-grained part of the sequence can be traced throughout the entire lake. This is interpreted as a late Glacial, transgressive facies, deposited during a lake level rise after the major lake level low stand of the Last Glacial

Maximum (LGM). The associated lake level high stand is documented by beach remains in the Nam Co catchment that have a minimum OSL age of 16.1 ka (Schütt et al. 2008). The analysed section from Nam Co contains the complete sediment record following probable desiccation at the core site.

Bulk and compound-specific geochemical variables (TC, TIC, CaCO_3 , TOC, TN, TOC/TN, *n*-alkanes, HI, OI, TS)

Bulk geochemical variables are used for qualitative understanding of hydrological conditions in lake

systems and variations in primary production, which are ultimately associated with climate changes (Fig. 6). The Nam Co sediments reveal total carbon (TC) contents between 5 and 9% and total organic carbon (TOC) ranging between 1 and 3%, with average values of 6.70 and 1.98%, respectively. The two variables do not show a parallel trend with depth, in contrast to the significant positive correlation between TC and TIC ($r = 0.88$), indicating that variations in TC are mainly due to changes in inorganic carbon (TIC). Carbonate content of the sediments varies between 25 and 62% (mean 40%) and ostracode valves probably account for much of the CaCO_3 . TIC in Nam Co is thought to represent mainly changes in primary production in the lake. TOC is strongly correlated with total nitrogen (TN) ($r = 0.88$), suggesting a common origin.

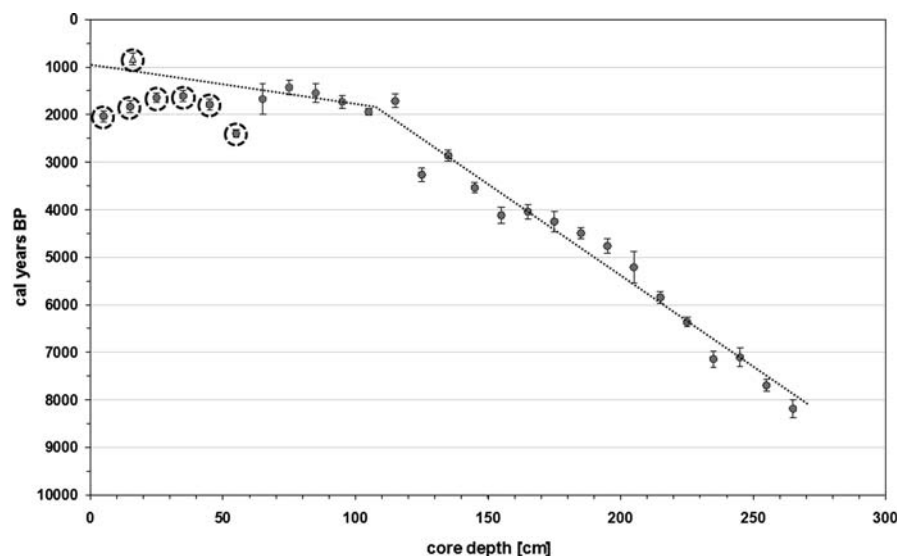
In general, concentrations of TOC and TN increase gradually by 1.5 to 0.1% at the core base, up to 2.5 and 0.3% at about 5.4 cal ka BP, while TC and TIC decrease. This increase in %TOC was likely caused by the decrease in TC and TIC, representing decreased dilution of TOC rather than an increase in productivity associated with rising lake level. Until 3.5 cal ka BP, TOC and TN tended to decrease continuously, while TC and TIC remained relatively stable. Between 3.4 and 1.0 cal ka BP, concentrations of TOC and TN again increase slightly, while inorganic carbon decreases. In the upper core section, organic and inorganic carbon content are highly variable and the concentrations rise to almost double previous values (Fig. 6).

Variables used to characterize organic matter (OM) sources ($C_{\text{org}}/N_{\text{total}}$ ratio, Hydrogen Index (HI), *n*-alkane distribution) indicate a predominantly aquatic origin throughout the sequence (Fig. 6). Previous studies in Nam Co showed long-chain *n*-alkanes with 27–31 carbon atoms come from terrestrial vegetation. Mid-chain *n*-alkanes with 21–23 carbon atoms are from aquatic macrophytes (Mügler et al. 2008).

n-Alkanes from aquatic sources far exceed the amount of long-chain, terrestrial components (Fig. 6). Mid-chain-length *n*-alkanes show maximum amounts around 6.2–5.4 cal ka BP and significantly elevated concentrations around 3 cal ka BP and between 1.4 cal ka and 500 cal years BP. The general down-core trend of *n*-alkane concentration is tracked by the %TOC, with lower concentrations between 5.4 and 1.8 cal ka BP (Fig. 6).

Lake phytoplankton and bacterial remains are typically rich in hydrogen and thus have high HI values (>300 HC/g TOC) (Meyers and Lallier-Verges 1999). HI values <150 mg HC/g TOC are typical for terrestrial-derived OM or bacterial degradation and oxidation (Tissot and Welte 1984). In a van Krevelen-type HI/OI discrimination plot, most of the Nam Co samples are located between the type II and type III OM field (Fig. 4). Type II OM originates from algae and is rich in hydrocarbons, while type III is poor in hydrocarbons and rich in carbohydrates and indicates woody plant material. Since the Nam Co OM is characterized as being of aquatic origin using

Fig. 2 Calibrated, uncorrected ^{14}C ages of Nam Co 8 bulk sediments (dots) and macro remain (triangle). Marked samples were not included in the linear regression for reservoir correction



n-alkane data, the trend of decreasing HI and increasing OI values suggests oxidation of type II OM. Oxidation decreases the hydrogen content while increasing the oxygen content, thus converting type II OM to type III (Meyers and Lallier-Verges 1999).

The source of OM in lacustrine sediments is often determined by the C_{org}/N_{total} ratio (Meyers and Ishiwatari 1993) (Fig. 6). Nam Co sediments do not reveal major shifts in C_{org}/N_{total} values, suggesting a rather constant OM source. Values range between 6 and 10, typical for lakes in which organic matter is from autochthonous algal production (Meyers and Ishiwatari 1993). In the lower core section, until 3.5 cal ka BP, C_{org}/N_{total} values are slightly higher, compared to the upper part. Higher values may reflect preferential loss of N from OM during degradation, and/or increased contribution of terrestrial OM.

Degradation of OM is often characterized by the Carbon Preference Index (CPI), which describes the ratio between odd and even carbon chain lengths of *n*-alkanes (Bray and Evans 1961; Marzi et al. 1993) (Fig. 6). Values >3 are typical for recent, or relatively unaltered OM. CPI values of the Nam Co sediments vary between 2 and 8, suggesting generally good preservation of OM. The lower core section, until 3.5 cal ka BP, is characterized by elevated CPI values (mean CPI: 7). The upper part has only a slightly lower value (mean CPI: 5.3), indicating good preservation throughout, and suggesting somewhat greater input of terrestrial material in the early part of the record (Fig. 6).

Stable carbon and hydrogen isotopes ($\delta^{13}C$ bulk and compound-specific $\delta^{13}C$ and δD)

Carbon stable isotope compositions are also used to infer OM source and the paleoproductivity of lakes (Meyers and Lallier-Verges 1999). $\delta^{13}C$ was measured on bulk organic matter and compound-specific *n*-alkanes. We present bulk $\delta^{13}C$ values, data from nC_{21} , representing *n*-alkanes of aquatic origin, and data from nC_{27} , representing *n*-alkanes from terrestrial sources (Fig. 7). $\delta^{13}C$ values of bulk organic matter vary between -26 and -22‰ , with a general trend to enrichment towards the core top. Differences in fractionation during photosynthesis allow discrimination of sediment OM sources. While terrestrial C_3 plants typically have $\delta^{13}C$ values of -28‰ , C_4 plants are higher, around -14‰ (Oleary 1988). Isotopic signatures on bulk OM in Nam Co sediments ($-24 \pm 0.8\text{‰}$) correspond to terrestrial C_3 plant material. Nevertheless, because lacustrine algae also use the C_3 Calvin pathway, the $\delta^{13}C$ of sediment bulk OM cannot discriminate between terrestrial C_3 plants and algae, especially if dissolved CO_2 in the lake is in isotopic equilibrium with the atmosphere (Meyers and Lallier-Verges 1999). Furthermore, the $\delta^{13}C$ of aquatic OM is influenced by the availability of dissolved CO_2 and can be altered by shifts in the $CO_2-HCO_3^-$ equilibrium caused by changes in pH of the lake water (Hassan et al. 1997).

Meyers and Lallier-Verges (1999) suggest isotope characterisation of OM in combination with TOC/TN ratio, which is independent of the photosynthetic pathway, to avoid misinterpretation of bulk $\delta^{13}C$ values. Most of the samples in the discrimination plot

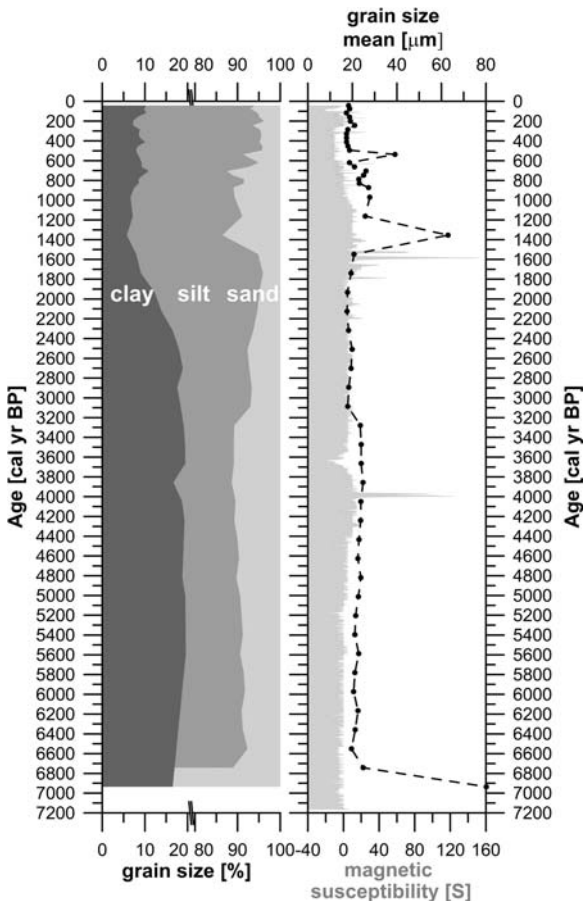


Fig. 3 Grain size distribution, magnetic susceptibility and grain size statistics. Note the break on the x-axes for grain size distribution

(Fig. 5) are located in the field for lacustrine algae. This matches the characterization of OM based on the TOC/TN values and Rock Eval analyses, and indicates that aquatic organisms are the main source of OM in Nam Co sediments.

Because OM sources have different *n*-alkane chain lengths, compound-specific $\delta^{13}\text{C}$ values can be determined independently for both aquatic and terrestrial plant material (Fig. 7). Mid-chain *n*-alkanes ($n\text{C}_{21}$ and $n\text{C}_{23}$) show a similar downcore trend and are significantly correlated ($r = 0.81$, $P < 0.005$). $n\text{C}_{21}$ has a mean $\delta^{13}\text{C}$ value of $-22.8 \pm 2.5\%$, consistent with observed values for aquatic plants of about $-25.3 \pm 2\%$ (Chikaraishi and Naraoka 2003). The long-chain *n*-alkane $n\text{C}_{27}$ (as well as $n\text{C}_{29}$ and $n\text{C}_{31}$) have more depleted mean $\delta^{13}\text{C}$ values of $-29.8 \pm 1\%$, reflecting terrestrial C_3 plant material (Chikaraishi and Naraoka 2003).

Relatively large down-core changes are only observed for $\delta^{13}\text{C}_{\text{bulk}}$ and the mid-chain *n*-alkanes, whereas long-chain *n*-alkane $\delta^{13}\text{C}$ shows only minor fluctuations (Fig. 7). This suggests that vegetation composition did not change during the last 7 cal ka and was dominated by C_3 plants. The mean $\delta^{13}\text{C}$ value from the aquatic *n*-alkane $n\text{C}_{21}$ changed from 20.8 to 25.1 ‰ during the last 1,000 cal years.

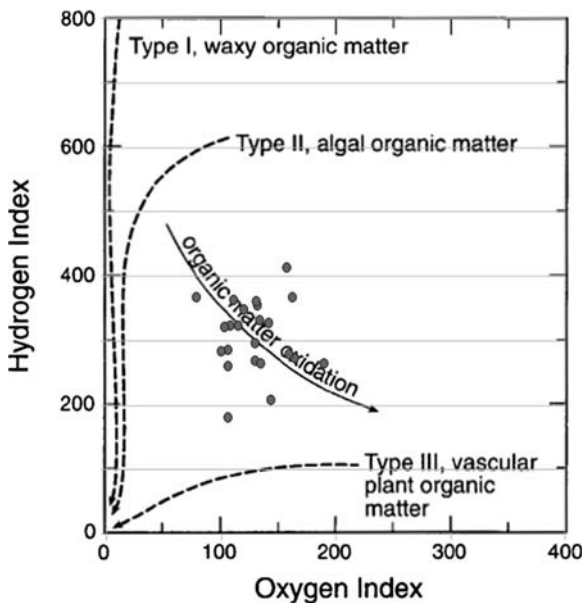


Fig. 4 Nam Co samples in a van Krevelen-type discrimination plot (after Meyers and Lallier-Verges 1999)

Whereas bulk $\delta^{13}\text{C}$ values and aquatic-derived $\delta^{13}\text{C}$ values show a weak, but significant correlation for this lower core section ($r = 0.52$; $P < 0.05$) and are correlated between 3.5 and 1.4 cal ka BP ($r = 0.63$; $P < 0.05$), the records are not correlated during the last 1,000 cal years. This suggests that variations in bulk $\delta^{13}\text{C}$ are not explained by aquatic *n*-alkanes, and bulk OM is a mix of terrestrial and aquatic organic matter.

Compound-specific δD values were measured on sediment *n*-alkanes (Fig. 7), as they are increasingly being used to reconstruct paleoclimatic and paleohydrological conditions (Sachse et al. 2004; Schefuss et al. 2005; Shuman et al. 2006). Downcore variations in δD of the aquatic *n*-alkanes are significantly correlated ($r = 0.51$; $P < 0.0001$). Likewise, downcore variations in terrestrial *n*-alkanes are significantly correlated ($r = 0.47$; $P < 0.0001$). For interpretation of δD values, we again use $n\text{C}_{21}$ to characterize aquatic *n*-alkanes and use $n\text{C}_{27}$ as a terrestrial biomarker. The two OM sources have significantly different δD values (*t*-test with $\alpha = 0.05$, $P < 0.005$), enabling differentiation between mid- and long-chain *n*-alkanes based on the hydrogen isotope signatures (Fig. 7). The terrestrial *n*-alkane ($n\text{C}_{27}$) shows very slightly enriched values in the lower core section, but no overall trend throughout ($-212 \pm 22\%$). There are, however, large excursions in δD , with variations up to 100‰. These are assumed to indicate changes in moisture source or precipitation regime, alternating between monsoonal rains and convective rains experiencing moisture recycling. These variations are consistent with the observed range of δD values from precipitation during the year at Nam Co (Keil et al. 2009). δD in the aquatic *n*-alkanes ($n\text{C}_{21}$) shows general isotope enrichment towards the top of the core. In addition to this general increase ($\sim 70\%$), variations in δD are interpreted to reflect short-term fluctuations between arid and humid climate conditions (Mügler et al. 2008).

The δD record of terrestrial and aquatic *n*-alkanes permitted identification of three main sedimentation periods: (1) 7.2–3.8 cal ka BP, when terrestrial *n*-alkanes are isotopically lighter than aquatic *n*-alkanes by $\sim 34\%$, which is comparable to observed values under mid-European humid climate conditions (Fig. 7), (2) 3.8–1.5 cal ka BP, when the concentration of terrestrial markers is too low for reliable δD determination. The mean δD value during this period from the aquatic *n*-alkanes is enriched by

~20‰ relative to the lower core section, and (3) since 1.5 cal ka BP, when terrestrial and aquatic *n*-alkanes have similar mean δD values (~−208 and −204‰), suggesting enrichment of the water source for aquatic *n*-alkanes, while input through precipitation remained stable.

Mineral composition

Quartz and other silicates in the lake deposits are predominantly allochthonous, eroded from the catchment and transported as suspended load (Fig. 8). Quartz and feldspar are mainly formed in magmatic rocks. Calcite is derived from weathering of calcium-bearing feldspars (hydrolysis). Higher water temperatures and increased pH values lower its solubility, leading to precipitation and sedimentation. High amounts of calcite may also be produced by biomineralization. In general, the concentrations of quartz and silicates reflect variability of weathering, runoff and erosion within the catchment. Authigenic formation of different forms of calcite and pyrite reflects changes in lake water chemistry, temperature and salinity. At Nam Co, calcite is also produced by ostracods, molluscs, eubacteria and cyanobacteria. A fairly rare mineral, monohydrocalcite (MHC), appears initially around 1.5 cal ka BP, and shows constant concentrations until recent times. There is some controversy about the mechanisms responsible for MHC formation. In addition to cold-water formation in, for example, spray zones of waterfalls (Fischbeck and Müller 1971), biological activity by

algae and other microorganisms is cited (Taylor 1975), and could be a factor in Nam Co.

The Nam Co 8 sediments contain allochthonous and authigenic minerals in nearly equal amounts (Fig. 8). A significant rise in allochthonous minerals starts ~2.7 cal ka BP and their abundance peaks between 1,500 and 800 cal years BP. Whereas the composition of allochthonous materials has not changed, minerals assumed to have been formed within the lake display significant variations. In general, precipitation of primary carbonate minerals is controlled by the availability of dissolved CO₂, and thus pH of the water column, evaporative concentration, as well as the mixing of brines of different concentrations (Last and Ginn 2005). Whereas the pH of the water column controls carbonate precipitation mainly in humid climates, concentration changes are dominant in arid climates. In addition, the cations in solution, usually expressed by the Mg/Ca ratio of the lake water, control which carbonate mineral is precipitated. Mg-calcite and dolomites precipitate with elevated Mg/Ca ratios (Last and Ginn 2005).

Sediment geochemistry—major elements

(Na, K, Mg, Fe, Mn, Ca, Sr, P, Al)

Variations in the content of Fe, Mn, Al and K are similar throughout the core, with slight discrepancies for Al in some depositional phases (Fig. 9). These four elements are interpreted as indicators of input from catchment sources. Allochthonous detrital material reaches the lake with fluvial runoff or via soil erosion or aeolian transport. Thus, these elements may show the strength of transport mechanisms. Further evidence that Fe is allochthonous is deduced from its ratio with Mn (Boyle 2001) (Fig. 9) and P (Engstrøm and Wright 1984). When Fe is formed authigenically within a lake, Fe is often enriched in surface sediments at the oxic/anoxic boundary or is present as Fe-carbonate (siderite). However, the comparison between Ca, Mg and Sr contents in the HCl and aqua regia digests showed that these elements reflect changes in the carbonate content. Association of Ca with sulphates is likely negligible because Ca-rich periods correlate with carbonate peaks. This is also supported by microscopic analysis of the >63- μ m fraction, that consists mainly of ostracode valves in the lower part of the core. Strontium is common in both sulphates and

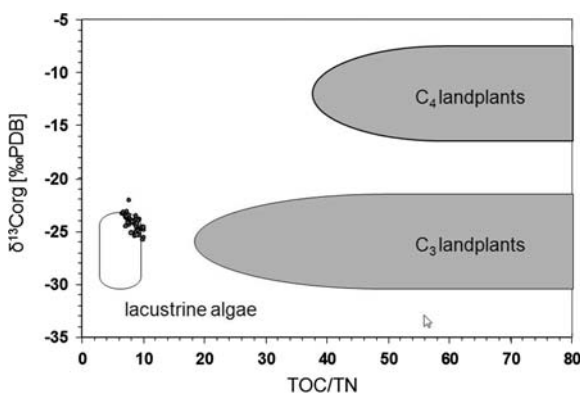


Fig. 5 Characterization of Nam Co organic matter source by plotting elemental and carbon isotopic composition of organic matter plotted (after Meyers and Lallier-Verges 1999)

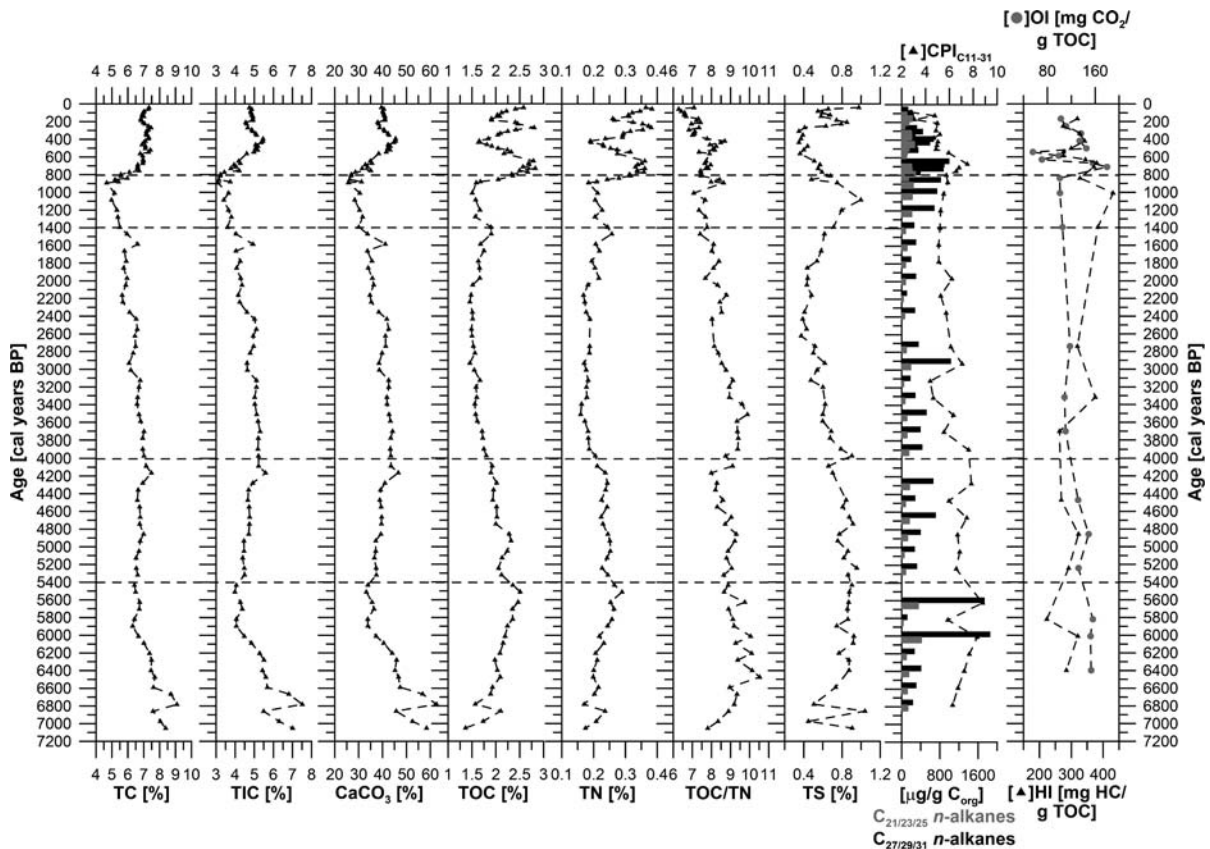


Fig. 6 Bulk geochemical variables and *n*-alkane concentrations from the Nam Co 8 core; CPI_{11-31} was calculated as $0.5 \times (\frac{\sum_{\text{odd}}}{\sum_{\text{even}}} + \frac{\sum_{\text{odd}}}{\sum_{\text{even}}})$

carbonates. Because it does not track variations in carbonate, deposition in sulphate cannot be ruled out, although gypsum was not detected. Similar to Mg, Sr probably substitutes for Ca in calcite, forming low- or high-Mg and -Sr calcites. If substitution of Ca by Mg or Sr is dependent on salinity, and if different ostracodes incorporate the elements in similar fashion, then the shifts in Mg and Sr in the upper part of the core can be ascribed to biogenic formation of calcite by algae. This is also supported by the occurrence of monohydrocalcite in this part of the core.

Magnesium and sodium show a continuous increase to the top of the core. As magnesium is derived from carbonate and sodium most likely from feldspar, their ratio may reflect both lake and catchment processes. Allochthonous contributions (via erosion from catchment soils) to the sediments may be assumed if there

was a positive correlation with C/N ratio (Simola 1983). Because this is not the case, we suggest that increases in both Mg and Na reflect increasing chemical enrichment of the lake water caused by a decline in volume. Differences in the occurrence of Mn, Na, K, Fe and Al may reflect changes in soil-forming processes or variable sources of allochthonous material. Phosphorus is widely used as an indicator for lake productivity because it is often the limiting nutrient (Engström and Wright 1984). Increased P concentrations are associated with anthropogenic activities such as land cultivation or sewage disposal (Håkanson and Jansson 1983). Within the Nam Co sediment core, P gradually increases. Sources of phosphorus within the catchment bedrock can be largely ignored. Increasing P content is ascribed to the increasing human activities within the study area, especially during the last 400 years.

Fig. 7 Bulk $\delta^{13}\text{C}$ values and compound-specific stable isotope ratios (δD and $\delta^{13}\text{C}$) from selected *n*-alkanes (see appendix Figs. 11 and 12 for all *n*-alkanes)

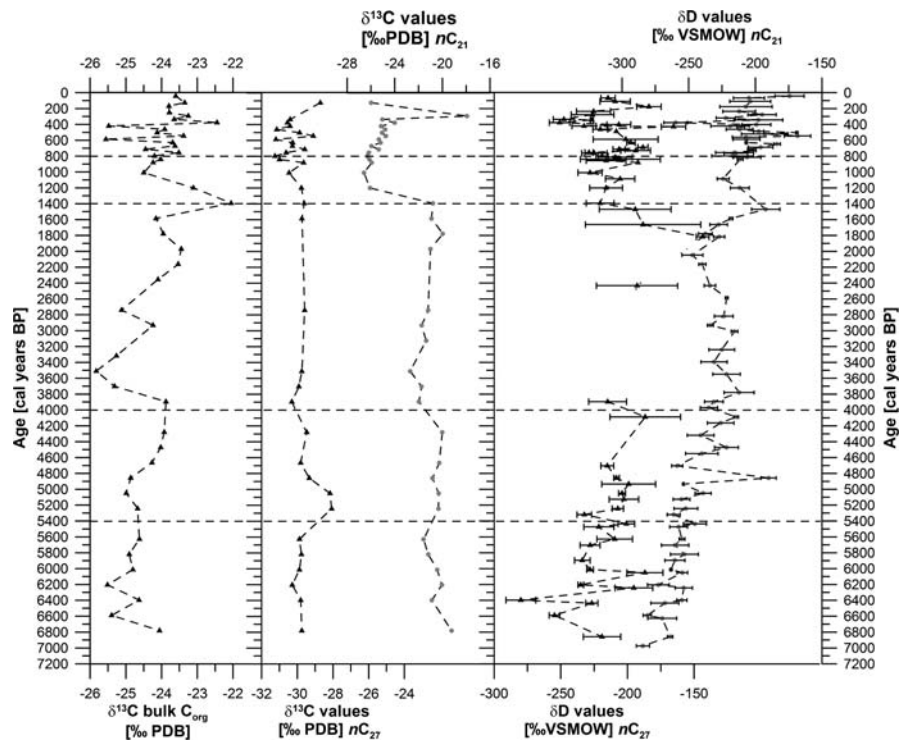
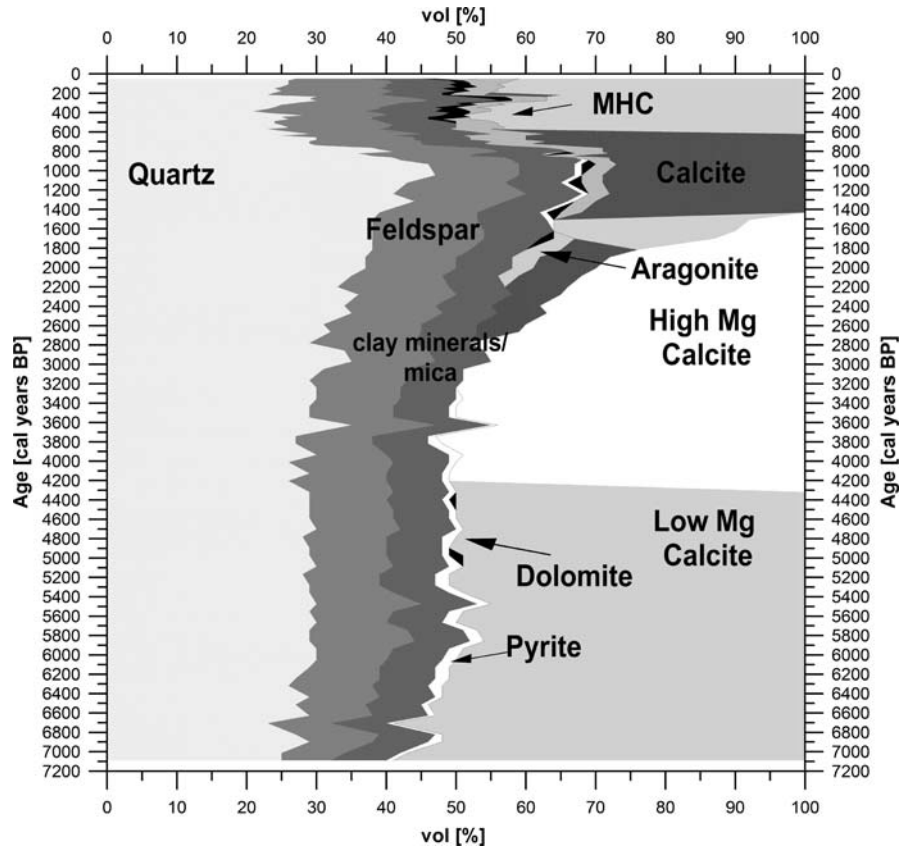


Fig. 8 Mineralogy of the Nam Co 8 core



Hydrological changes inferred from Nam Co lake sediments

We used geochemical and mineralogical variables (Figs. 6, 7, 8) to divide the Nam Co 8 core into five depositional units. Sedimentation began at least $7,237 \pm 193$ cal years BP, when lake level was maximal. Subsequent deposition occurred as the lake shrank and salinity increased.

Unit I (~ 7.2 to ~ 5.4 cal ka BP)

This sedimentation phase is characterized by increases in Fe, K and Al (Fig. 9). Since these elements are major constituents of silicate minerals, they are attributed to the allogenic fraction being eroded from catchment soils and rocks (Engström and Wright 1984). High runoff and weathering led to increased transport of clastic material and deposition in Nam Co, implying humid climate conditions and a positive water balance. The positive correlation between Fe and TOC ($r = 0.95$) as well as Fe and Al ($r = 0.95$) could imply transport of Fe as organic complexes after the solution of Fe in reduced soils, due to waterlogging or build-up of humus at the soil

surface (Engström and Wright 1984). Furthermore, the similarity between the Fe/Mn ratio and Fe content (Fig. 9) indicates a higher rate of Fe supply during this depositional stage (Boyle 2001). In addition, slightly increasing TOC/TN ratios suggest higher input of allochthonous OM (Fig. 6). Increasing TN and TOC concentrations may either reflect enhanced supply of soil-derived organic matter, or rising OM production from both terrestrial and aquatic sources, since concentrations of aquatic and terrestrial *n*-alkanes increase during this time period. Alternatively, increased TN and TOC may be explained by decreased TC and TIC, i.e. reduced dilution of TOC and TN as a consequence of rising lake level. Low-Mg-calcite is precipitated during this stage (Fig. 8). It is less soluble than carbonate minerals aragonite, calcite and high-Mg-calcite. Occurrence of this CaCO_3 form could imply an increased water supply, as melt water from surrounding glaciers, or as runoff from higher precipitation, leading to dilution of the other minerals (Müller et al. 1972). Alternatively, as proposed by Bayon et al. (2007), low-Mg calcite may be of biogenic origin, formed by infaunal organisms such as ostracodes, which are abundant during this interval.

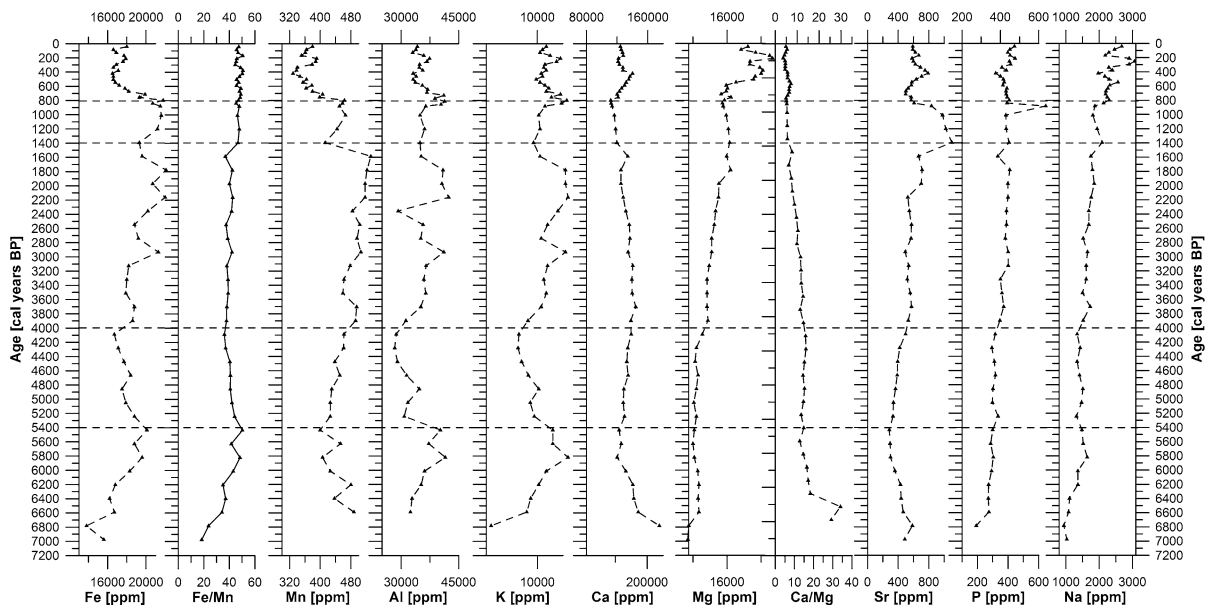


Fig. 9 Major geochemical data of Nam Co 8 sediments

Aquatic (nC_{21}) n -alkanes show the most depleted δD values in this unit, with a mean of -262‰ (Fig. 7). Subsequent deuterium enrichment of the aquatic biomarker was probably a consequence of diminishing water volume in Nam Co, so this period represents the highest lake levels in the sequence. Terrestrial n -alkane (nC_{27}) δD values show their most negative values (mean -224‰), indicating hydrogen from an isotopically light source such as melt water or intense monsoonal rains (Fig. 6). Using the modern, observed fractionation factor between precipitation and terrestrial n -alkanes in the study area ($\sim 100\text{‰}$) (Mügler et al. 2008), we infer a mean precipitation signal of -138‰ during this interval, which is considerably depleted compared to the present annual mean of -122‰ (Keil et al. 2009). In addition, we observe an isotopic difference of $\sim 36\text{‰}$ between the terrestrial nC_{27} and aquatic nC_{21} n -alkane δD values, which is consistent with values from mid-European humid climates where precipitation and inflow exceed the output through evaporation and outflow (Sachse et al. 2004) (Fig. 7). Thus, sedimentation during Unit I occurred under humid conditions, with potentially pronounced monsoonal precipitation and a high contribution of runoff and/or melt water input to the lake.

Unit II (~ 5.4 to ~ 4 cal ka BP)

During this depositional stage, most elements and minerals display minor variations or relatively constant values. Only Fe, Al and K decrease upcore, which is attributed to reduced input of catchment material mobilized from soils or rock weathering (Fig. 9). We characterize this period as more or less stable with respect to environmental conditions, although the slight increase of Na, Ca, and Mn may suggest diminishing water volume and increasing salinity. Low-Mg calcite is again the carbonate mineral precipitated (Fig. 8). This indicates that the environmental conditions within the lake did not change significantly during Unit II and low Mg/Ca ratios (<2) are inferred for the lake water (Müller et al. 1972). Both terrestrial and aquatic biomarker δD values show a trend towards enriched values during this time interval. The increase in deuterium content of the long-chain component from terrestrial sources could be attributed to a diminishing contribution of melt water from the

surrounding glaciers, to decreased monsoonal rainfall, or to an increase in air temperature. Enrichment in nC_{21} is even more pronounced, suggesting increased evaporation of lake water. During Unit II, lake hydrology and chemistry were controlled by decreased precipitation or melt water inflow that reduced erosion input into the lake, and by higher evapotranspiration rates. The lake volume was shrinking.

Unit III (~ 4.0 cal ka BP to ~ 1.4 cal ka BP)

Most variables continued trends established in the previous depositional stage. TOC, TN, TIC and Ca remained constant (Fig. 6) and the elements that characterize slight, but ongoing salinization such as Mg, Na, Sr gradually increased, with simultaneous decreasing Ca/Mg and Ca/Sr ratios. Elevated Fe, Al and K contents (Fig. 9), which are associated with allochthonous input, were probably not a consequence of high runoff. Instead, they are thought to have originated from reworked material from the lake shore, through wave activity. Alternatively, low rainfall could have caused less vegetation cover on the soil surface, leading to increased sediment input during high precipitation events. Material reworking is suggested as the correlation between Al, Fe and TOC is no longer significant, which implies that dissolved metals were transported in association with soil organics (Engstrøm and Wright 1984). Reduced input from terrestrial sources is also inferred from lower concentrations of long-chain n -alkanes during this interval. Gradually decreasing TOC/TN ratios suggest increasing importance of aquatic OM, as indicated by higher concentrations of mid-chain n -alkanes as well (Fig. 6). In addition, precipitation of high-Mg calcite in the lower part of the core section implies elevated Mg/Ca ratios in the lake water (2–12) associated with higher salinities, indicating lake shrinkage (Fig. 8) (Müller et al. 1972). Lower lake levels are also indicated by elevated Mn concentrations that point to oxidation of the hypolimnion and effective water column mixing (Yancheva et al. 2007). Parallel precipitation of calcite, aragonite and high-Mg calcite in the upper part of Unit III indicates major fluctuations of water volume, providing further evidence for reworking of material from the lake shore (Müller et al. 1972).

Both δD and $\delta^{13}\text{C}$ values of $n\text{C}_{21}$, as well as $\delta^{13}\text{C}$ of bulk OM show isotope enrichment, indicating that aquatic plants grew in lake water concentrated by evaporation (Meyers and Lallier-Verges 1999) (Fig. 7). Since $\delta^{13}\text{C}$ values of the long-chain components maintain constant values of $\sim -30\text{‰}$ (although shown only for four data points), we rule out vegetation changes (i.e. C_3 to C_4 plants) as a control on the stable isotope signatures. Data density for δD values from the terrestrial marker ($n\text{C}_{27}$) is too low during this time to specify the processes controlling enrichment of lake water. However, the $n\text{C}_{27}$ δD values within this unit suggest significant enrichment in hydrogen isotopes, up to $\sim -144\text{‰}$, and using the modern fractionation value (Mügler et al. 2008), yields precipitation δD values that today are only observed during periods when convective rainfall occurs after evaporation of lake surface water (Keil et al. 2009). In general, climate during this interval was semi-arid to arid and was driest around 1.6–1.4 cal ka BP. This interval is characterized by negative water balance. Evaporation exceeded inputs, leading to the diminishing of the water reservoir and lower lake level compared to the previous unit.

Unit IV (~ 1.4 cal ka BP to ~ 800 cal years BP)

This period is characterized by a major change in grain size distribution from clay to silt and sand as the dominant particle sizes, associated with an increase in sedimentation rate (Figs. 2, 3). The lower part of Unit IV is characterized by negative shifts in Fe, Al, Mn and K, indicators for allochthonous detrital input (Fig. 9). This decrease could imply reduced runoff or dilution of these elements as a consequence of a rising lake level through increased precipitation and runoff. There is an increase in allogenic minerals that originate from the surrounding catchment (Fig. 8). Because the solubility of the above mentioned elements is strongly dependent on pH and rises with increasing acidity (Engström and Wright 1984; Håkanson and Jansson 1983), we suggest that increased runoff led to greater input of soil-derived humic substances into the lake, which reduced pH and thus favoured their solution. The occurrence of pyrite and the reduced precipitation of calcite (Fig. 8) and Ca concentrations further suggest the acidity of lake

water (Last and Ginn 2005; Müller et al. 1972; Simola 1983). Increased lake acidity would also support the hypothesis of increased contribution of soil organic substances, making ^{14}C ages too old in this Unit (Fig. 2). There is a depletion of mean δD values in $n\text{C}_{27}$ long-chain n -alkanes of $\sim 17\%$, from -192 to -209 , while δD values of mid-chain n -alkanes ($n\text{C}_{21}$) are enriched when compared to the previous unit, though continued enrichment within this interval is not apparent. Concentrations of Mg and Na are fairly stable and may suggest dilution during a period with a positive lake water balance. A possible lake level rise in this period, however, is not supported by Sr values, which could be explained by a change in the incorporation of Sr into calcite due to higher contributions from algae than from ostracodes (Keatings et al. 2002).

Lake level increase is also suggested by higher S concentrations, presumed to indicate reducing conditions, as well as by the significant depletion of $\delta^{13}\text{C}$ in $n\text{C}_{21}$. Sediments in this interval were most likely deposited during humid climate conditions, under a positive lake water balance.

Unit V (since ~ 800 cal years BP)

The period since 800 cal years BP is characterized by lake shrinkage, expressed by increases in Na and Mn and the lowest Ca/Mg ratios of the entire sequence. This indicates the lowest water volume and a maximum in salinity (Fig. 9). Elements from allochthonous sources (Fe, Mn, Al, K) and allogenic minerals decrease, implying less erosional transport due to reduced precipitation and runoff. Carbonates besides low-Mg calcite include monohydrocalcite (MHC), known to originate from chemical precipitation and biological activity in the Nam Co sediments (Li et al. 2008) (Fig. 8). Alkaline conditions ($\text{pH} > 8$) are necessary to produce and preserve MHC, thus its presence indicates a highly evaporative environment.

δD values of terrestrial and aquatic n -alkanes show large fluctuations ($\sim 60\text{‰}$) compared to previous units. Large isotope fluctuations can be caused by changes in water source or precipitation regimes, e.g. convective rains that are isotopically heavier due to moisture recycling, and monsoonal precipitation, which is depleted in deuterium (Fig. 7). Overall, δD values of the long-chain component show isotopically

depleted values with a mean of -211‰ , while δD values from $n\text{C}_{21}$ continue the trend of isotope enrichment. Continued enrichment of the aquatic biomarker supports the hypothesis of decreasing lake level and implies high evaporation rates leading to a negative water balance. This is further supported by the fact that δD values of the aquatic marker are enriched compared to the terrestrial components, and indicates arid climate conditions (Mügler et al. 2008).

Although there is a general trend of lake volume reduction since 800 cal years BP, we also observe short-term excursions in most of the variables around 450 cal years BP that point to humid climate, and at ~ 200 cal years BP when exceptionally dry conditions are inferred. These changes may correspond to effects of the Little Ice Age in Europe, a climate phenomenon that is known to be associated with stronger and weaker monsoon activity (Zhang et al. 2008). Recent climate conditions started ~ 100 cal years BP with increasing lake shrinkage. Since that time, Na and Mg, as well as the Mg/Ca ratio, gradually increased again, and the aquatic biomarker $n\text{C}_{21}$ shows enriched δD values. Unfortunately, uppermost samples in the core are lacking, thus the modern observed increase in the level of Nam Co is not covered in our dataset (You et al. 2006).

Implications for the Tibetan Plateau paleoenvironmental history

To incorporate the Nam Co lacustrine record into the broader hydrological and climatological perspective on the Tibetan Plateau, we compared our data to records from other lake systems (Figs. 1, 10). Bangong Co (Gasse et al. 1991) and the Sumxi–Longmu Co lake system (Avouac et al. 1996; Fontes et al. 1993; Gasse et al. 1991) were supposedly located within the influence of the Indian monsoon during the Holocene. Selin Co (Gu et al. 1993) is a large saline lake under the influence of the summer monsoon today, and Cuo Co (Wu et al. 2006b), which is located on the Central Tibetan Plateau, is closest to Nam Co. In addition, Lake Qinghai, at the NE margin of the Tibetan Plateau, is considered to be influenced by the south-eastern monsoon (Lister et al. 1991; Shen et al. 2005). For this comparison, we compiled the published records on the mineralogical and organic composition of sediments, stable isotopic signature

of carbonates, biological indicators, and pollen records. We then inferred past hydrological changes and defined wet and dry periods. For classification, we differentiated the climate characteristics into eight categories, where “1” represents exceptionally dry conditions and “8” represents very wet conditions. Temperature is not considered as a factor in our scheme. In general, wet periods reflect times of increasing lake level or high rainfall. Dry periods characterize phases where evaporation exceeds precipitation and lake level declines.

Warmer and wetter climate conditions than those of today—early to mid Holocene

The Nam Co record starts ~ 7.2 cal ka BP. Thus, the major shift from cool and dry to warmer and wetter climate conditions between 10.8 and 9.6 ka BP, reported for the lakes mentioned above, is not recorded in the Nam Co 8 sediments. The basal part of the Nam Co 8 core is not yet analysed and dated, but consists of coarse sands that are interpreted as transgressive facies deposited during a period of rising lake level. This may reflect a humid period with intensified monsoonal precipitation. Wet and warm conditions associated with intensified monsoon circulation remained until around 6.3–6.0 ka BP at Bangong Co (Gasse et al. 1996) and Sumxi–Longmu Co, until around 5.5 ka BP at Selin Co, until 5.7 ka BP at Cuo Co, and until 4.5 ka BP at Lake Qinghai (Shen et al. 2005). Maximum intensities of monsoonal precipitation, associated with highest lake levels and the maximum extent of monsoonal circulation, are recorded at all sites between 6.5 and 5.5 ka BP. Generally, this period of favourable environmental conditions is termed the Holocene Optimum. Within the Nam Co 8 sediments, we record the remainder of the climate optimum until around 5.4 cal ka BP, summarized in depositional *Unit 1*. From 6.2 to 5.7 ka BP marks the end of the Holocene hydrological and climate optimum, with a precipitation/evaporation deficit reflected in the enrichment of $\delta^{18}\text{O}$ values at Bangong Co and Sumxi–Longmu Co. At Lake Qinghai, environmental proxies indicate the termination of the Holocene Optimum ~ 6 cal ka BP (Shen et al. 2005). The termination of the early to mid-Holocene humid climate conditions at the different lake sites shows movement of the

monsoonal precipitation boundary towards the southeast. This implies a gradual decrease in rainfall intensity and a weakening of the southern monsoons during the early Holocene, first affecting Bangong Co and Sumxi–Longmu Co in the NW, and afterwards the central and southern lakes, including Nam Co. The gradual retreat of high precipitation intensity in a southeasterly direction is confirmed by the stable isotope records of the Linxia basin, situated SE of Nam Co, and Lake Daihai in east China. At those sites, the Holocene Optimum is recorded until ~ 5 cal ka BP (Fan et al. 2007) and 3.6 cal ka BP (Sun et al. 2006), respectively.

Increasing aridity during the mid-Holocene

After the highest lake levels are recorded with the Holocene Optimum, lake levels began to gradually decrease indicating a general trend towards aridity.

This trend started at Bangong Co and Sumxi–Longmu Co around 6.0 ka BP, lasted until 3.8 ka BP, and terminated in an extreme dry period around 3.2 ka BP. Starting about 500 years later at Cuo Co and Selin Co, maximum aridity was reached at the same time, around 3.3–3.0 ka BP (Gasse et al. 1996; Wu et al. 2006a). Selin Co sediments indicate a transition period until ~ 4.5 cal ka BP and a first aridity maximum between ~ 4.2 and ~ 3.3 ka BP that is coincident with a pronounced dry period at Nam Co around ~ 3.7 cal ka BP. Lake Qinghai also shows maximum aridity around 3.9 cal ka BP (Shen et al. 2005). Records from Bangong Co and Sumxi–Longmu Co indicate increased aridity between 3.8 and 3.2 ka BP. The contemporaneous occurrence of pronounced dry climate conditions could indicate the 4.2-ka event which is documented in a number of natural climate archives in Asia (Arz et al. 2006; Staubwasser et al. 2003) as well as monsoonal Africa (Booth et al. 2005; Gasse 2000). Although the causes

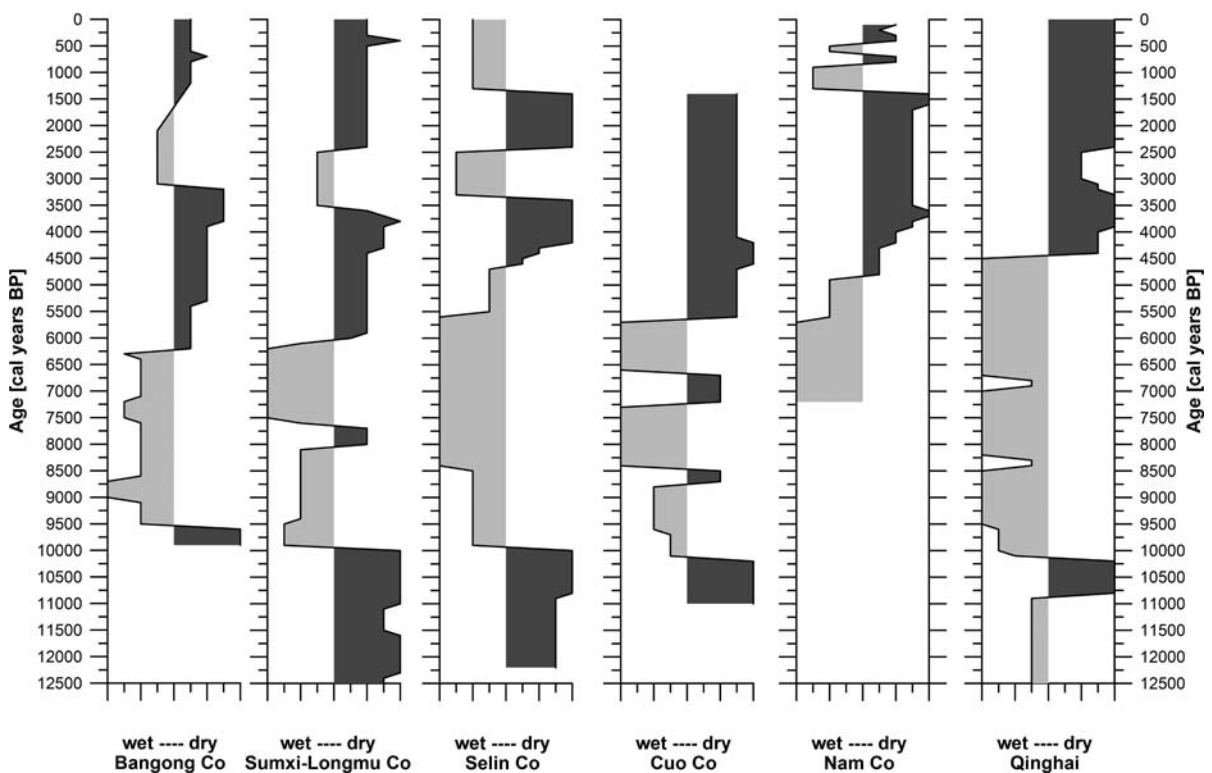


Fig. 10 Comparison of wet and dry periods inferred from lake records across the Tibetan Plateau

of the 4.2-ka event remain unknown, some authors suggest external forcing and solar variability induced weakening monsoonal circulation. A moister period of minor amplitude is recorded for Bangong Co, Sumxi–Longmu Co and Selin Co between ~ 3.5 and ~ 2.1 ka BP (Gasse et al. 1996). Lacustrine sediments of Cuo Co and Nam Co and the Qinghai record indicate arid climate conditions (Shen et al. 2005; Wu et al. 2006a). The significant moisture in the western lakes, and the minor impact at Nam Co, Cuo Co, and Qinghai Lake located on the Central Plateau and eastern region, suggest this wet interval was caused by air masses originating from the Westerlies. Afterwards, the records clearly indicate increased aridity. Selin Co and Nam Co sediments show episodes of much greater dryness between ~ 2.4 and ~ 1.4 ka BP and at ~ 1.5 cal ka BP, respectively. This suggests that climate effects were felt at smaller spatial scales and may imply a particularly weak southern monsoon during this period.

Late-Holocene and modern climate conditions

Correlation of the establishment of modern climate conditions among systems is challenging because of chronological uncertainties in the records. Although aridity appears to continue at Bangong Co, Sumxi–Longmu Co, and Lake Qinghai (Gasse et al. 1996; Shen et al. 2005), the record from Selin Co indicates moister conditions from 1.4 ka BP to present (Gasse et al. 1996). At Nam Co the sediment record also indicates increased precipitation and runoff between ~ 1.4 and ~ 800 cal yr BP, followed by generally drier conditions, which are interrupted by shorter-duration humid and very arid periods that may correspond to the Little Ice Age. These wet and dry episodes were probably associated with stronger and weaker southern monsoons, respectively.

Conclusions

The Nam Co 8 sediment core provides insights into the paleoenvironmental history of the Tibetan Plateau since ~ 7.2 cal ka BP. During the middle and late

Holocene, the lake system and its catchment experienced changes between pronounced humid and arid climate conditions that caused lake level increases and decreases, respectively. These lake level shifts were ultimately controlled by monsoonal moisture availability and evapotranspiration. The basal part of the core was deposited under transgressive conditions that started >7.2 cal ka BP when summer monsoonal circulation strengthened rapidly on the Tibetan Plateau, leading to a warmer and wetter climate. The long-term trend towards aridity was initiated between ~ 5.8 and ~ 4.2 cal ka BP and culminated in two pronounced dry episodes at ~ 3.7 and ~ 1.5 cal ka BP. Drying may have been associated with the 4.2-ka event recorded widely in monsoonal Asia. After a marked wet spell from 1,400 to 800 cal years BP that might be associated with the Medieval Warm Period, lake shrinking proceeded gradually, associated with a decrease in monsoonal rain intensity and increasing mean air temperatures. Comparison of the Nam Co record with other lake records across the Tibetan Plateau shows overall agreement in paleohydrological evolution. The timing of the termination of the Holocene Climate Optimum suggests gradual movement of the southern monsoonal precipitation boundary in a southeasterly direction and implies a gradual decrease in rainfall intensity related to a weakening of the southern monsoon. Major events around 8 ka and the ~ 4.2 -ka dry event appear across the Tibetan Plateau. These events are also recorded in monsoonal Africa, India and China, which implies they were caused by large-scale changes in energy redistribution of the ocean-atmosphere-land system. A comprehensive picture of the establishment of modern climate conditions for the last 2,000 years remains incomplete because of poor chronological control in some records, and in some cases lake desiccation, which led to a loss of the paleoenvironmental archive. A detailed compilation of lake records across the Tibetan Plateau, which includes the most recent period of the Holocene, is essential to evaluate late Holocene behaviour of the Asian monsoon system.

Acknowledgments We thank the German Research Foundation (DFG), which supported this research with grant GI-262-11. We also acknowledge the Institute of Tibetan Plateau Research (ITPR-CAS) for scientific, data and logistical

support. A special thanks is given to John Wallner and Ernst Kroemer for retrieving the sediment core and to Peter Frenzel with whom we had several fruitful discussions. We also would like to thank the editor for improving the article in terms of language and grammar.

Open Access This article is distributed under the terms of the Creative Commons Attribution Noncommercial License which permits any noncommercial use, distribution, and reproduction

in any medium, provided the original author(s) and source are credited.

Appendix

See Figs. 11 and 12.

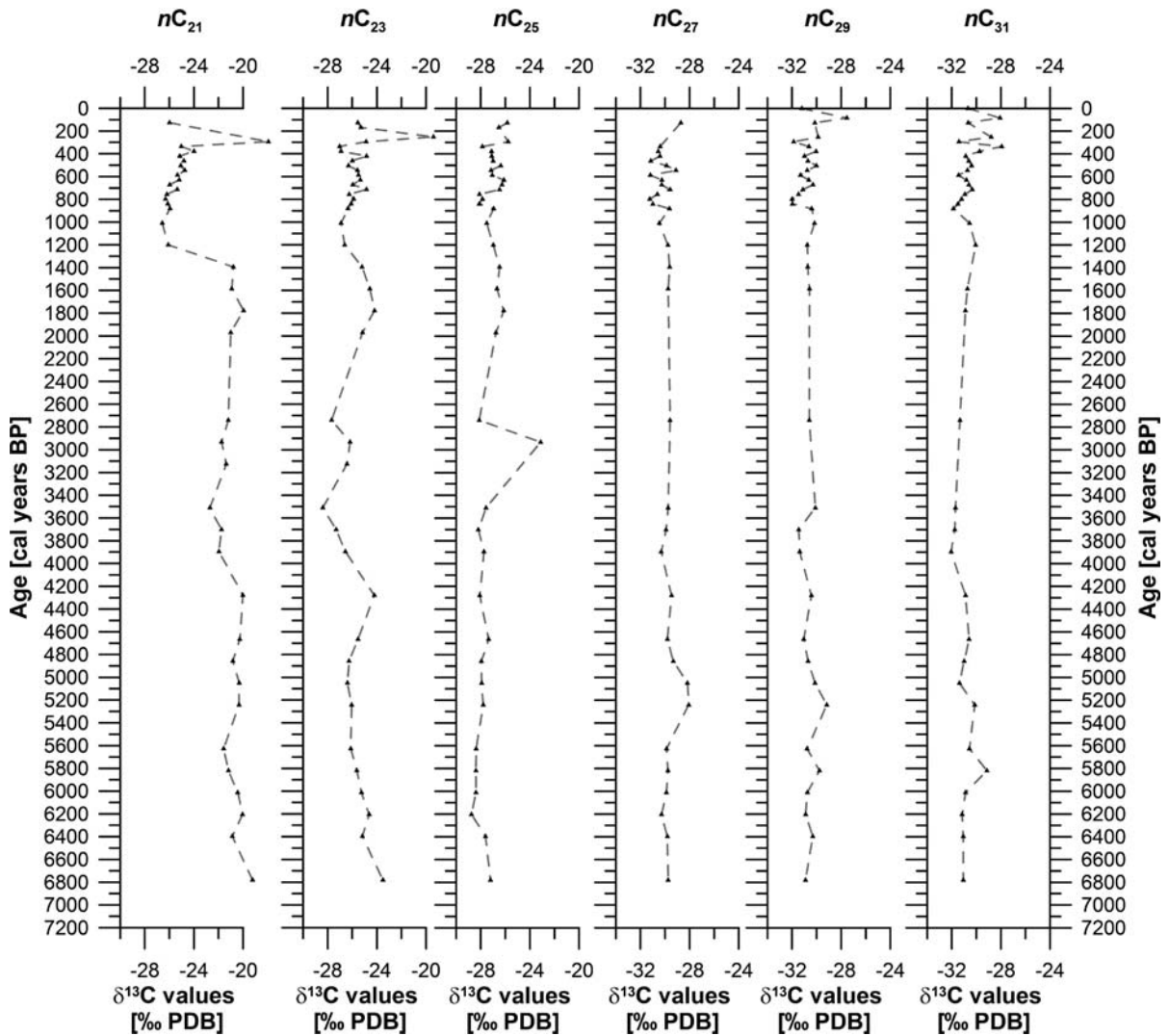


Fig. 11 Carbon isotope content of individual alkanes from the core

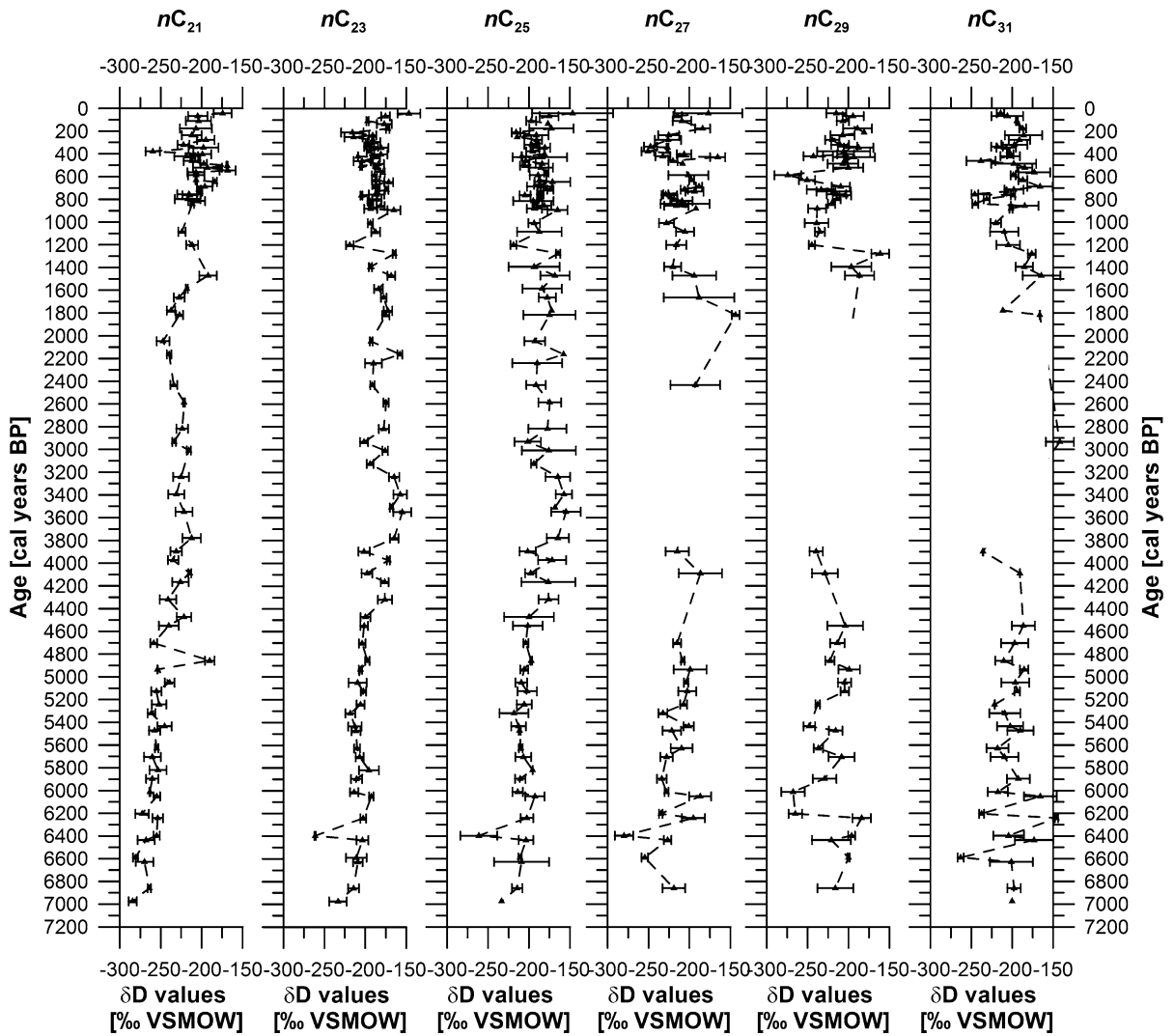


Fig. 12 Hydrogen isotope content of individual alkanes from the sediment core

References

An Z, Porter SC, Kutzbach JE, Xihao W, Suming W, Xiaodong L, Xiaoqiang L, Weijian Z (2000) Asynchronous Holocene optimum of the East Asian monsoon. *Quaternary Sci Rev* 19:743–762

Arz HW, Lamy F, Patzold J (2006) A pronounced dry event recorded around 4.2 ka in brine sediments from the northern Red Sea. *Quaternary Res* 66:432–441

Avouac JP, Dobremez JF, Bourjot L (1996) Palaeoclimatic interpretation of a topographic profile across middle Holocene regressive shorelines of Longmu Co (western Tibet). *Palaeogeogr Palaeoclimatol Palaeoecol* 120:93–104

Baas M, Pancost R, van Geel B, Damste JSS (2000) A comparative study of lipids in *Sphagnum* species. *Org Geochem* 31:535–541

Bayon G, Pierre C, Etoubleau J, Voisset M, Cauquil E, Marsset T, Sultan N, Le Drezen E, Fouquet Y (2007) Sr/Ca and Mg/Ca ratios in Niger Delta sediments: implications for authigenic carbonate genesis in cold seep environments. *Mar Geol* 241:93–109

Booth RK, Jackson ST, Forman SL, Kutzbach JE, Bettis EA, Kreig J, Wright DK (2005) A severe centennial-scale drought in mid-continental North America 4200 years ago and apparent global linkages. *Holocene* 15:321–328

Boyle JF (2001) Inorganic geochemical methods in paleolimnology. In: Last W, Smol JP (eds) *Tracking environmental change using lake sediments, physical and geochemical methods*. Kluwer, Dordrecht, pp 83–142

Bray EE, Evans ED (1961) Distribution of normal-paraffins as a clue to recognition of source beds. *Geochim Cosmochim Acta* 22:2–15

- Bronk Ramsey C (2001) Development of the radiocarbon calibration program. *Radiocarbon* 43:355–363
- Chen FH, Cheng B, Zhao Y, Zhu Y, Madsen DB (2006) Holocene environmental change inferred from a high-resolution pollen record, Lake Zhuyeze, arid China. *Holocene* 16:675–684
- Chikaraishi Y, Naraoka H (2003) Compound-specific δD - δC^{13} analyses of *n*-alkanes extracted from terrestrial and aquatic plants. *Phytochemistry* 63:361–371
- Craig H (1961) Isotopic variations in meteoric waters. *Science* 133:1702–1703
- Cranwell PA, Eglinton G, Robinson N (1987) Lipids of aquatic organisms as potential contributors to lacustrine sediments.2. *Org Geochem* 11:513–527
- Dansgaard W (1964) Stable isotopes in precipitation. *Tellus* 16:436–468
- Dykoski CA, Edwards RL, Cheng H, Yuan D, Cai Y, Zhang M, Lin Y, Qing J, An Z, Revenaugh J (2005) A high-resolution, absolute-dated Holocene and deglacial Asian monsoon record from Dongge Cave, China. *Earth Planet Sc Lett* 233:71–86
- Eglinton G, Hamilton RJ (1967) Leaf epicuticular waxes. *Science* 156:1322
- Engström DR, Wright HD (1984) Lake sediments and environmental history. In: Tutin W, Haworth EY, Lund JWG (eds) *Studies in palaeoecology in honour of Winifred Tutin*. University of Minnesota Press, Minneapolis, pp 11–63
- Espitalie J, Deroo G, Marquis F (1985) Rock-eval pyrolysis and its applications. *Rev I Fr Petrole* 40:563–579
- Fan MJ, Dettman DL, Song CH, Fang XM, Garzione CN (2007) Climatic variation in the Linxia basin, NE Tibetan Plateau, from 13.1 to 4.3 Ma: the stable isotope record. *Palaeogeogr Palaeoclimatol Palaeoecol* 247:313–328
- Ficken KJ, Li B, Swain DL, Eglinton G (2000) An *n*-alkane proxy for the sedimentary input of submerged/floating freshwater aquatic macrophytes. *Org Geochem* 31:745–749
- Fischbeck R, Müller G (1971) Monohydrocalcite, hydromagnesite, nesquehonite, dolomite, aragonite, and calcite in speleothems of Fränkische Schweiz, Western Germany. *Contrib Mineral Petr* 33:87–93
- Fontes JC, Melieres F, Gibert E, Qing L, Gasse F (1993) Stable isotope and radiocarbon balances of two Tibetan Lakes (Sumxi Co, Longmu Co) from 13,000 BP. *Quaternary Sci Rev* 12:875–887
- Fontes JC, Gasse F, Gibert E (1996) Holocene environmental changes in Lake Bangong basin (western Tibet) 1. Chronology and stable isotopes of carbonates of a Holocene lacustrine core. *Palaeogeogr Palaeoclimatol Palaeoecol* 120:25–47
- Gao YX (1985) Tibetan soil. *Science, Beijing*, pp 2–15 (in Chinese)
- Gasse F (2000) Hydrological changes in the African tropics since the Last Glacial Maximum. *Quaternary Sci Rev* 19:189–211
- Gasse F, Arnold M, Fontes JC, Fort M, Gibert E, Huc A, Li BY, Li YF, Lju Q, Melieres F, Vancampo E, Wang FB, Zhang QS (1991) A 13,000-year climate record from Western Tibet. *Nature* 353:742–745
- Gasse F, Fontes JC, Vancampo E, Wei K (1996) Holocene environmental changes in Bangong Co basin (western Tibet) 4. Discussion and conclusions. *Palaeogeogr Palaeoclimatol Palaeoecol* 120:79–92
- Gehre M, Geilmann H, Richter J, Werner RA, Brand WA (2004) Continuous flow H^2/H^1 and O^{18}/O^{16} analysis of water samples with dual inlet precision. *Rapid Commun Mass Sp* 18:2650–2660
- Gu ZY, Liu JQ, Yuan BY, Liu DS, Liu RM, Liu Y, Yaskawa K (1993) Monsoon variations of the Qinghai-Xizang Plateau during the Last 12,000 years—geochemical evidence from the sediments in the Siling Lake. *Chinese Sci Bull* 38:577–581
- Håkanson L, Jansson M (1983) *Principles of lake sedimentology*. Springer, Berlin, p 316
- Hassan KM, Swinehart JB, Spalding RF (1997) Evidence for Holocene environmental change from C/N ratios, $\delta^{13}C$ and $\delta^{15}N$ values in Swan Lake sediments, western Sand Hills, Nebraska. *J Paleolimnol* 18:121–130
- Herzschuh U (2006) Palaeo-moisture evolution in monsoonal Central Asia during the last 50,000 years. *Quaternary Sci Rev* 25:163–178
- Herzschuh U, Winter K, Wünnemann B, Li SJ (2006) A general cooling trend on the central Tibetan Plateau throughout the Holocene recorded by the Lake Zigetang pollen spectra. *Quatern Int* 154:113–121
- Hilkert AW, Douthitt CB, Schlüter HJ, Brand WA (1999) Isotope ratio monitoring gas chromatography mass spectrometry of D/H by high temperature conversion isotope ratio mass spectrometry. *Rapid Commun Mass Sp* 13:1226–1230
- Johnson KR, Ingram BL (2004) Spatial and temporal variability in the stable isotope systematics of modern precipitation in China: implications for paleoclimate reconstructions. *Earth Planet Sc Lett* 220:365–377
- Kapp JLD, Harrison TM, Kapp P, Grove M, Lovera OM, Lin D (2005) Nyainqentanglha Shan: a window into the tectonic, thermal, and geochemical evolution of the Lhasa block, southern Tibet. *J Geophys Res Sol Ea* 110:B08413. doi: 10.1029/2004JB003330
- Keatings KW, Heaton THE, Holmes JA (2002) Carbon and oxygen isotope fractionation in non-marine ostracods: results from a 'natural culture' environment. *Geochim Cosmochim Acta* 66:1701–1711
- Keil A, Berking J, Mügler I, Schütt B, Schwalb A, Steeb P (2009) Hydrological and geomorphological basin and catchment characteristics of Lake Nam Co, South-Central Tibet. *Quatern Int.*, (in press)
- Last W, Ginn F (2005) Saline systems of the Great Plains of western Canada: an overview of the limnogeology and paleolimnology. *Saline Sys* 1:10
- Lehmkuhl F, Haselein F (2000) Quaternary paleoenvironmental change on the Tibetan Plateau and adjacent areas (Western China and Western Mongolia). *Quatern Int* 65/66:121–145
- Lehmkuhl F, Klinge M, Rees-Jones J, Rhodes EJ (2000) Late Quaternary aeolian sedimentation in central and south-eastern Tibet. *Quatern Int* 68:117–132
- Leng MJ, Marshall JD (2004) Palaeoclimate interpretation of stable isotope data from lake sediment archives. *Quaternary Sci Rev* 23:811–831
- Li MH, Kang SC, Zhu LP, You QL, Zhang QG, Wang JB (2008) Mineralogy and geochemistry of the Holocene

- lacustrine sediments in Nam Co, Tibet. *Quatern Int* 187:105–116
- Lister GS, Kelts K, Zao CK, Yu JQ, Niessen F (1991) Lake Qinghai, China—closed-basin lake levels and the oxygen isotope record for ostracoda since the latest Pleistocene. *Palaeogeogr Palaeoclimatol Palaeoecol* 84:141–162
- Marzi R, Torkelson BE, Olson RK (1993) A revised carbon preference index. *Org Geochem* 20:1303–1306
- McCarthy RD, Duthie AH (1962) A rapid quantitative method for the separation of free fatty acids from other lipids. *J Lipid Res* 3:117–119
- Meyers PA, Ishiwatari R (1993) Lacustrine organic geochemistry—an overview of indicators of organic-matter sources and diagenesis in lake-sediments. *Org Geochem* 20: 867–900
- Meyers PA, Lallier-Verges E (1999) Lacustrine sedimentary organic matter records of Late Quaternary paleoclimates. *J Paleolimnol* 21:345–372
- Miehe G, Miehe S, Schlutz F, Kaiser K, Duo L (2006) Palaeoecological and experimental evidence of former forests and woodlands in the treeless desert pastures of Southern Tibet (Lhasa, AR Xizang, China). *Palaeogeogr Palaeoclimatol Palaeoecol* 242:54–67
- Morrill C (2004) The influence of Asian summer monsoon variability on the water balance of a Tibetan lake. *J of Paleolimnol* 32:273–286
- Morrill C, Overpeck JT, Cole JE (2003) A synthesis of abrupt changes in the Asian summer monsoon since the last deglaciation. *Holocene* 13:465–476
- Morrill C, Overpeck JT, Cole JE, Liu KB, Shen CM, Tang LY (2006) Holocene variations in the Asian monsoon inferred from the geochemistry of lake sediments in central Tibet. *Quaternary Res* 65:232–243
- Mügler I, Sachse D, Werner M, Xu B, Wu G, Yao T, Gleixner G (2008) Effect of lake evaporation on δD values of lacustrine *n*-alkanes: a comparison of Nam Co, Tibetan Plateau and Holzmaar, Germany. *Org Geochem* 39: 711–729
- Müller G, Irion G, Förstner U (1972) Formation and diagenesis of inorganic Ca-Mg carbonates in the lacustrine environment. *Naturwissenschaften* 59:158–164
- Oleary MH (1988) Carbon isotopes in photosynthesis. *Bio-science* 38:328–336
- Radke M, Willsch H, Welte DH (1980) Preparative hydrocarbon group type determination by automated medium pressure liquid-chromatography. *Anal Chem* 52:406–411
- Sachse D, Radke J, Gleixner G (2004) Hydrogen isotope ratios of recent lacustrine sedimentary *n*-alkanes record modern climate variability. *Geochim Cosmochim Ac* 68: 4877–4889
- Sachse D, Radke J, Gleixner G (2006) δD values of individual *n*-alkanes from terrestrial plants along a climatic gradient - Implications for the sedimentary biomarker record. *Org Geochem* 37:469–483
- Schefuss E, Schouten S, Schneider RR (2005) Climatic controls on central African hydrology during the past 20,000 years. *Nature* 437:1003–1006
- Schütt B, Berking J, Frechen M, Yi C (2008) Late Pleistocene lake level fluctuations of the Nam Co, Tibetan Plateau, China. *Z Geomorph NF Suppl Bd* 2:57–74
- Shen J, Liu XQ, Wang SM, Matsumoto R (2005) Palaeoclimatic changes in the Qinghai Lake area during the last 18,000 years. *Quatern Int* 136:131–140
- Shuman B, Huang YS, Newby P, Wang Y (2006) Compound-specific isotopic analyses track changes in seasonal precipitation regimes in the Northeastern United States at ca 8200 cal yr BP. *Quaternary Sci Rev* 25:2992–3002
- Simola H (1983) Limnological effects of peatland drainage and fertilization as reflected in the varved sediment of a deep lake. *Hydrobiologia* 106:43–58
- Smith FA, Freeman KH (2006) Influence of physiology and climate on δD of leaf wax *n*-alkanes from C₃ and C₄ grasses. *Geochim Cosmochim Ac* 70:1172–1187
- Smittenberg RH, Eglinton TI, Schouten S, Damste JSS (2006) Ongoing buildup of refractory organic carbon in boreal soils during the Holocene. *Science* 314:1283–1286
- Staubwasser M, Sirocko F, Grootes PM, Segl M (2003) Climate change at the 4.2 ka BP termination of the Indus valley civilization and Holocene south Asian monsoon variability. *Geophys Res Lett* 30:1425. doi:10.1029/2002GL016822
- Steinhof A, Adamiec G, Gleixner G, van Klinken GJ, Wagner T (2004) The new ¹⁴C analysis laboratory in Jena, Germany. *Radiocarbon* 46:51–58
- Sun QL, Zhou J, Shen J, Chen P, Wu F, Xie XP (2006) Environmental characteristics of Mid-Holocene recorded by lacustrine sediments from Lake Daihai, north environment sensitive zone, China. *Sci China Ser D* 49: 968–981
- Taylor GF (1975) Occurrence of monohydrocalcite in two small lakes in southeast of south-Australia. *Am Mineral* 60:690–697
- Thompson LG, Mosley-Thompson E, Davis ME, Mashiotta TA, Henderson KA, Lin PN, Yao TD (2006) Ice core evidence for asynchronous glaciation on the Tibetan Plateau. *Quatern Int* 154:3–10
- Tian LD, Yao TD, MacClune K, White JWC, Schilla A, Vaughn B, Vachon R, Ichiyonagi K (2007) Stable isotopic variations in west China: a consideration of moisture sources. *J Geophys Res Atmos* 112:4293
- Tissot B, Welte DH (1984) Petroleum formation and occurrence. Springer, Berlin, p 699
- Wang J, Zhu L (2006) Preliminary study on the field investigation of Nam Co. Annual report of Nam Co monitoring and research station for multisphere interactions. ITPR-CAS, Beijing, p 42
- Williams WD (1991) Chinese and Mongolian saline lakes—a limnological overview. *Hydrobiologia* 210:39–66
- Wu YH, Lücke A, Jin ZD, Wang SM, Schleser GH, Battarbee RW, Xia WL (2006a) Holocene climate development on the central Tibetan Plateau: a sedimentary record from Cuoe Lake. *Palaeogeogr Palaeoclimatol Palaeoecol* 234:328–340
- Wu YH, Wang SM, Hou XH (2006b) Chronology of Holocene lacustrine sediments in Co Ngoin, central Tibetan Plateau. *Sci China Ser D* 49:991–1001
- Wu JL, Schleser GH, Lücke A, Li SJ (2007) A stable isotope record from freshwater lake shells of the eastern Tibetan Plateau, China, during the past two centuries. *Boreas* 36:38–46

- Wünnemann B, Chen FH, Riedel F, Zhang CJ, Mischke S, Chen GJ, Demske D, Ming J (2003) Holocene lake deposits of Bosten Lake, southern Xinjiang, China. *Chinese Sci Bull* 48:1429–1432
- Wünnemann B, Mischke S, Chen FH (2006) A Holocene sedimentary record from Bosten Lake, China. *Palaeogeogr Palaeoclimatol Palaeoecol* 234:223–238
- Xu S, Zheng GD (2003) Variations in radiocarbon ages of various organic fractions in core sediments from Erhai Lake, SW China. *Geochem J* 37:135–144
- Yancheva G, Nowaczyk NR, Mingram J, Dulski P, Schettler G, Negendank JFW, Liu JQ, Sigman DM, Peterson LC, Haug GH (2007) Influence of the intertropical convergence zone on the East Asian monsoon. *Nature* 445:74–77
- Yao TD, Shi YF, Thompson LG (1997) High resolution record of paleoclimate since the little ice age from the tibetan ice cores. *Quatern Int* 37:19–23
- You Q, Kang S, Li C, Li M and Liu J (2006) Features of meteorological parameters at Nam Co station, Tibetan Plateau. Annual report of Nam Co monitoring and research station for multisphere interactions 1:8–15
- Zhai Q, Guo Z, Li Y, Li R (2006) Annually laminated lake sediments and environmental changes in Bashang Plateau, North China. *Palaeogeogr Palaeoclimatol Palaeoecol* 241:95–102
- Zhang W, Cui ZJ, Li YH (2006) Review of the timing and extent of glaciers during the last glacial cycle in the bordering mountains of Tibet and in East Asia. *Quatern Int* 154:32–43
- Zhang P, Cheng H, Edwards RL, Chen F, Wang Y, Yang X, Liu J, Tan M, Wang X, Liu J, An C, Dai Z, Zhou J, Zhang D, Jia J, Jin L, Johnson KR (2008) A test of climate, sun, and culture relationships from an 1810-Year Chinese cave record. *Science* 322:940–942
- Zhu L, Wang J, Lin X, Ju J, Xie M, Li MC, Wu Y, Daut G, Mäusbacher R, Schwab A (2007) Environmental changes reflected by core sediments since 8.4 ka in Nam Co, Central Tibet of China. *Quaternary Sci* 27:588–597